2010:138 CIV

MASTER'S THESIS

Reinforced Nanocomposites for Electrical Applications

Maxime Roux

Luleå University of Technology

MSc Programmes in Engineering
Materials Technology (EEIGM)
Department of Applied Physics and Mechanical Engineering
Division of Polymer Engineering

2010:138 CIV - ISSN: 1402-1617 - ISRN: LTU-EX--10/138--SE

ABB Corporate Research Center
Segelhofestrasse 1K
5405 Baden-Dätwill
SWITZERLAND

Luleå University of Technology (LTU)
Department of applied physics and mechanical engineering
971 87 Luleå
SWEDEN

MASTER'S THESIS

Reinforced Nanocomposites For Electrical Applications

Maxime ROUX
Students in 5th year the EEIGM
From February 1st, 2010 until July 31st, 2010

Supervised by **Dr Sian F. Fennessey**
ABB Corporate Research Center, Insulation and Polymer Technology (V2)

And **Lennart Wallström**
LTU Luleå tekniska Universitet, Department of Applied Physics and Mechanical engineering,
Polymer Engineering

EEIGM
European School of Material Sciences and Engineering
Rue Bastien Lepage
54 000 Nancy
France

ABSTRACT

This project is focused on studying the effects of particles for improving mechanical and thermal properties of glass fiber reinforced epoxy composite. Submicro and nanosized particle filled composites based on diglycidyl-ether of bisphenol A and anhydride-curing agents are evaluated. The particles examined in this report are Particle 1 (P1 – 700nm) supplied in powder; Particle 3 (P3 – 100nm), Particle 2 (P2 – 70nm), and Particle 4 (P4 – 45nm) supplied in masterbatches. These particles have been successfully used in laminates with clean woven E-glass fabric produced by vacuum assisted resin transfer molding (VARTM). Optical microscope and scanning electron microscope is used to observe the particles and the composites. Laminates of unfilled resin and unidirectional unwashed glass fabric are manufactured by wet lay.

When the particles or the masterbatch are mixed with the epoxy resin, the viscosity is increased significantly. Dynamic mechanical analyses of the epoxy and nanocomposite plates and their corresponding laminates show an increase of the storage modulus with the addition of particles, especially beyond Tg. The relative permittivity was always higher than the reference epoxy for the filled resins and more especially for laminates at 40°C. The laminates with 30vol% atlas 1/7 clean glass fabrics exhibit better results than the non-clean E-glass fabric (1). The dielectric dissipation factor was lower for the laminates with 30vol% clean glass fabric than for the matrix only, the laminates with 30vol% of ML clean fabric and atlas 1/7 normal fabric. The flexural strength is measured, and the most interesting results were found for the laminates with 30vol% atlas clean glass fabrics with 35,3wt% P3 particles in epoxy and with reference epoxy. Concerning the flexural strength of the matrices, the most interesting were found to be 143MPa for the epoxy filled with 12,6wt% P4 particles (45nm).

Electrical breakdown setup was built to test flat laminate of 4mm in a SF_6 gas chamber. Three types of samples were tested, samples with only matrix of the reference epoxy, samples with P3 particles filled epoxy plate and laminate of reference epoxy with 30vol% of clean atlas glass fabric.

Particles 5 (P5 – 15/30nm) supplied in masterbatch are also introduced in this project but the mixing is revealed to be more difficult than with the previous masterbatches and no more work was carried out at this stage.

AKNOWLEDGMENTS

I would like to thank all the permanent employees and interns working in the Insulation and Polymer technology group at the ABB Corporate Research Center, Baden-Dättwil, Switzerland, for the help and advice given during these 6 months and the excellent working ambiance.

I also want to thank supervisor Lennart Wallström at the LTU for giving me the opportunity to make my master thesis.

My thanks go also to Dr Sian F. Fennessey not only for supervising and making this project possible but also for all the knowledge I learnt during this internship.

TABLE OF CONTENTS

1. INTRODUCTION

This study focuses on the optimization of thermal conductivity for improving the heat dissipation in insulating material and the reduction of residual stresses during the processing of fiber reinforced composites. The effect of submicron and nano ceramic particles on the mechanical, dielectric and thermal properties, and on the processability of the epoxy resin system with and without fiber as reinforcement has been investigated. In this report, the ceramic particles investigated are the Particle 1 (P1 – 700nm) supplied in powder; Particle P3 (P3 – 100nm), Particle P2 (P2 – 70nm), Particle P4 (P4 – 45nm) and Particle P5 (P5 – 15/30nm) all supplied in masterbatches. Another important goal is to examine the affect of nano composites material on the interface and delamination on E-glass reinforced epoxy. The last goal is to develop a new breakdown strength measurement method in order to characterize fiber reinforced nanocomposites plates in a SF_6 gas chamber.

Figure 1 : Hollow composite insulators

2. STATE OF THE ART

2.1. Epoxy resin

What is an epoxy Resin

Epoxy resin comes from a thermoset reaction between a resin and a hardener (amine or acid anhydride). The first plastic produced from epoxy family was synthesized from bisphenol A and Epichlorohydrin in the late 1930's by Dr Pierre Castan in Switzerland and Dr S.O. Greenlee in the United States. The main aspect of these materials is the terminal epoxide groups (2).

2.1.1. Epoxy Resin

An epoxy resin is a low molecular weight monomer produced from the base-catalyzed step-growth reaction of an epoxide with a dihydroxyl compound. One of the most common epoxies used is the diglycidyl ether of bisphenol A (DGEBA) which is the reaction between the bisphénol A and the epichlorohydrin (Figure 2) (2).

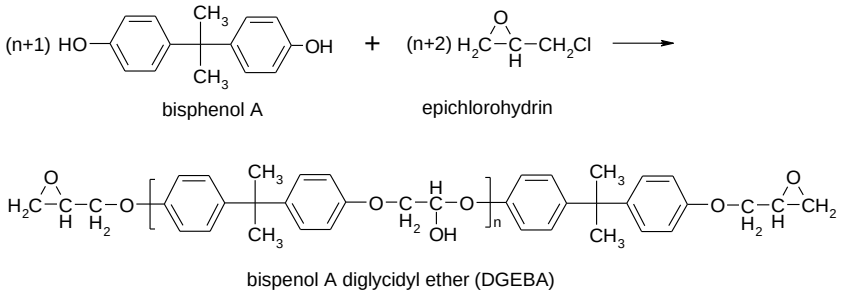

Figure 2 : Formation of DGEBA

2.1.2. Hardener

The hardener reacts with the epoxy resin in order to create a 3-dimensional network. This compound can be either an amine or an anhydride. Amines are mainly polyamines which create a ring opening of the epoxide group through a nucleophilic reaction. This kind of hardener will not be used in this report. Then, the second type of hardener is the anhydride which reacts with hydroxyl groups in order to form ester acid. Afterwards they can react with other ester or epoxy groups for producing new ester group. This hardener is the most used in the field of electrical industry thanks to their stability at low temperature (between 20 and 40°C), the low exothermic cross linkage and the very good thermal aging stability given to the final resin. The main disadvantage of this class of hardener is the low glass temperature which is around 110 – 120°C (2).

2.1.3. Accelerator

The aim of this chemical is to speed up the formation of the resin when the need is to get very quickly the material or to start the reaction at low temperature. They are often tertiary amines (R_3N) or Boron trifluorure (BF_3). When the resin and the hardener are mixed together,

the amine group from the hardener reacts with the epoxy group from the resin in order to form a covalent bond. Some other components can be added in the formulation like flexibilizators (2).

2.2. Insulators

An insulator is a electrical component designed to maintain or support an electrical conductor. Insulators are mainly found on power lines and power plants where the concentration of current is the highest. In power lines carrying the electricity, they isolate the electric current between the pylon and the conductive wires.

2.2.1. Materials and shape

For many years in the past, the insulators have been produced in glass and then in ceramic material. Nowadays, those materials are slowly being replaced by composite polymer material.

Those are typically composed of a central rod made of glass fiber reinforced polymer and the outer shed is made of silicon rubber (Figure 3). The insulators for outdoor use are designed to maximize the length of leakage path from one end to the other. In order to achieve this, the insulator is molded into a series of concentric disk shape (Figure 3).

In the case of gas-insulated live tank circuit breaker, the insulator should wishtand decomposed SF_6 gas. The glass fibers on the inner surface of the insulator are protected from the effect of SF_6 decomposition products by an epoxy liner reinforced with polyester fibers.

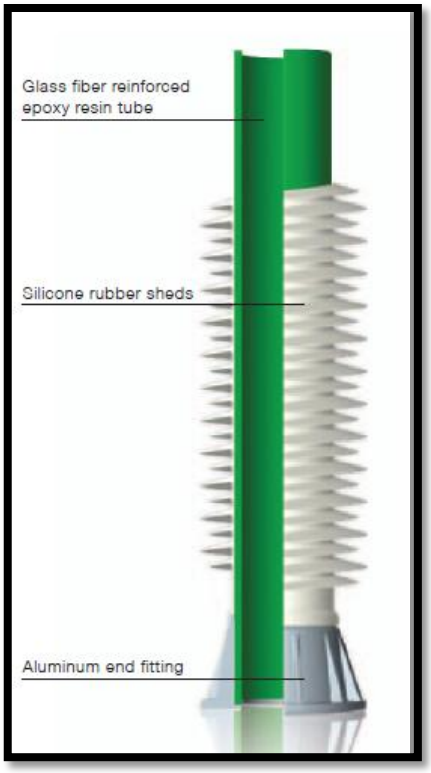

Figure 3 : Hollow core composite Insulator - ABB Composite Insulators commercial booklet (3)

2.2.2. Manufacturing

The FRP (Fibers reinforced plastic) tubes are produced using a winding machine. The glass fibers which have been pre-impregnated with resin are wound onto the mandrel and placed in an oven for curing (Figure 4a). The housing made from silicone is extruded, cured, bonded to the FRP tube (Figure 4b).

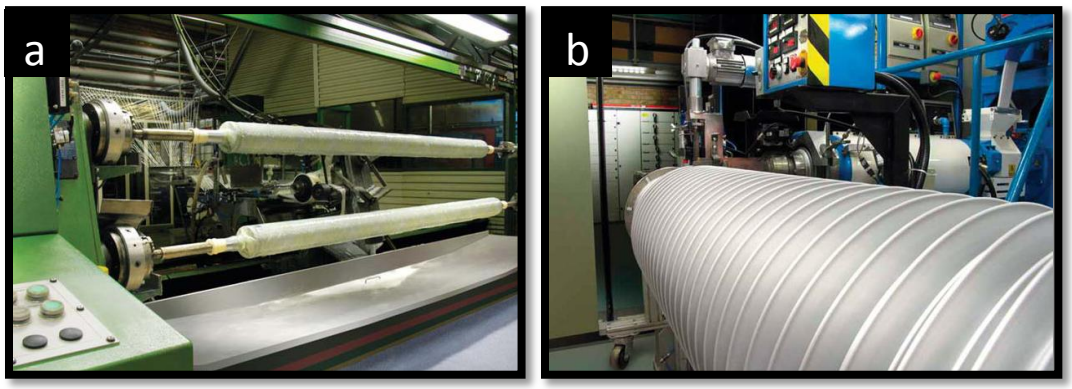

Figure 4 : a: Winding machine for the production of FRP tubes - b: extrusion of the silicon housing onto the tube

2.3. Fillers and particles

Conventional fillers in polymers are used mainly in order to reduce the final cost and to modify one or many of the properties of the material for particular applications. Indeed, often the use of such fillers will affect electrical properties such as dielectric strength and loss in a negative way. The enhancement of the mechanical properties is one of the most wanted achievement when fillers are added to the polymer matrix. The fillers are supplied in a broad number of shapes such as flakes, fibers, spherical particles. The shape of the fillers can also affect the final properties of the material. For example this property is also linked to the surface area of each particle. Some problems limit the use of fillers in the polymer industry. The viscosity of the uncured resin can be increased significantly which lead to a limitation of the content of fillers depending on the processing. The dispersion of the particles is one of the most important parameters which can affect significantly the final properties of the material. Moreover, when the fillers are added to a glass fabric reinforced polymer, the impregnation of the particle through the glass mats is also a critical parameter which can lead to a bad homogeneity and consequently lower properties for the final material. When a glass mat is used as reinforcement, the particles are sometimes filtered during impregnation.

2.3.1. Ceramic particles affect the mechanical and thermal properties

Ceramic particles are the best candidate for increasing thermal and mechanical properties especially with polymer matrix. Adding only a small amount of particles can increase the mechanical properties of an epoxy resin. Interlaminar shear strength is a matrix dominant property. When glass fabrics are used as reinforcement in an epoxy resin, the adhesion between the glass fibers and the polymer matrix is an important factor. This behavior is defined as the interlaminar shear strength. Wishman (4) reported that in glass mats reinforced epoxy resin with only 0,5wt% of silica nanoparticles (7nm), the best value for interlaminar shear was found for low fraction of glass fiber (37 vol%) and was up to 36MPa. This study revealed that as the fiber volume increase, the interlaminar shear decreases. This state is very important for our project. Moreover, Haque (5) by adding only 1% by weight of nanosilicate increase the interlaminar shear strength of a glass/epoxy clay nanocomposites of 44%. It has been reported that the use of fillers can affect in a good way the flexural strength of an epoxy resin. With the addition of only silica in the polymer matrix, the flexural strength is increased. Kornmann (6)

investigated the effect of silica nanoparticles (10wt %) on the flexural strength and modulus of a glass woven reinforced epoxy (54vol %) and these properties was improved of 27% and 6% respectively compared to the same material without nanoparticles. Many studies reported the same enhancement of mechanical properties when silica nanoparticles were added to an epoxy resin (7).

Mahrholz (7) made an epoxy resin reinforced with various content of silica particles and reported a reduction of the thermal expansion (about 30%) and an increase of the thermal conductivity (15%). The boron nitride particles (BN) exhibit a very important improvement of the thermal conductivity in epoxy resin (8). This improvement was greater than for many particles as nano alumina, diamond, nano beta-SiC, and nano amorphous Si_3N_4 usually used as reinforcement in epoxy resin (9). One of the explanation of this improvement with hexagonal micro boron nitride particles was due to their three dimensional structure compared to platelets (10). The morphology of fillers in epoxy resin plays an important role in the case of heat conduction. Liang (11) investigated the hexagonal Boron nitride with flakes and spherical shapes reinforced epoxy resin (DGEBA). Spherical BN particle increase the thermal conductivity twice more than the platelets.

2.3.2. Ceramic particles affect the dielectric properties

The dielectric properties are divided into several values which are the relative permittivity and the dielectric dissipation factor (tan δ). For a dielectric reinforced with particles or fibers, the increase of dielectric constants can be caused by interfacial polarization which formed electric charge at the interfaces (12). Krivda (13) measured a permittivity of 6 and a tan δ of 8.10^{-3} for 40vol% glass fiber reinforced epoxy. Many researchers reported that as the concentration of ceramic nanoparticles in epoxy resin increases the dielectrics properties decreases (14). This fact is critical in the case of material like insulators whom the first function is to be insulating. The challenge when particles are added to the neat resin is to increase the mechanical and thermal properties without decreasing the dielectric properties. Nowadays this state is not totally true because, it is possible to add particle and improve the dielectric properties considering the work of Zhao (15) which reported that when alumina nanoparticles are incorporated in neat epoxy, the dielectric constant was improved. The same situation has been described by Zhang (16) with BN platelet. Fothergill performed dielectric spectroscopy on epoxy nanocomposites containing various types of nano and micro fillers of TiO_2, Al_2O_3 and ZnO. He described a real improvement of the relative permittivity of ZnO from micro to nano size. Compared to the neat resin, permittivity was lower for nanofilled epoxy and higher for microfilled epoxy. (17)

The reinforcement of epoxy resin with E-glass fabrics leads to an enhancement of the mechanical properties and thermal conductivity (1) but also to reduction of the permittivity. The thermal conductivity of E-glass is 13W.m/K (18)

2.4. Interlaminar shear

The interlaminar shear is an important property for composite composed of overlaid layers. An interlaminar failure of laminates is the separation of two layers of a composite by

means of crack growing in the matrix between the two layers (Figure 5). The interlaminar shear strength represents the value when a composite starts producing this displacement between two laminates along the plane of their interface. Three modes of failure can be attributed to delamination (Figure 6); the mode 1 is defined by two forces acting perpendicularly to the layers and pulling apart the two layers. Mode two is defined as shear force operating in between the layers and making them slide over each other. Mode three creates shear forces in the plane perpendicular to mode 2.

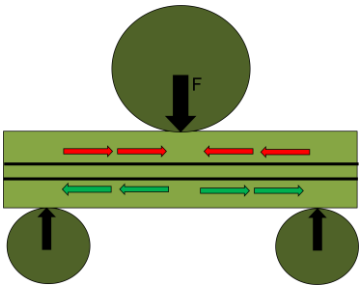

Figure 5 : Interlaminar shear created by the short beam method

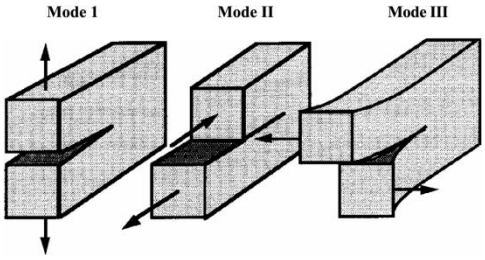

Figure 6 : Modes of interlaminar shear failure

2.4.1. Short beam method using 3 points bending

The short beam shear test refers to the standards ISO 14130:1997 (19) and ASTM D2344 (20) (Table 1). Rectangular samples are cut from the plates. The short beam shear test is similar to the 3-points bending test used to determine the flexural strength (Figure 7). In order to increase the level of shear stress at the expense of flexural stress, a smaller span/specimen thickness ratio is selected (4 or 5). Uni-directional fibers should be perpendicular to the loading nose. The sample is loaded at a strain rate of 1mm/min. The value of the interlaminar shear strength corresponds to the highest value of stress (N/mm^2) measured during this test when delamination occurs. The only mode of failure must be single or multiple interlaminar shear failures without any flexural deformation in compression and tension or any plastic deformation (Figure 8).

Methods presented:	Properties measured	Load	Standard
Short beam method using 3-point bending	Apparent shear	**Compression**	*ISO 14130:1997* (19) *ASTM D2344* (20)
±45° Tensile Test	In-plane shear	**Tension**	*ISO 14129* *ASTM D3518*
The V-Notched Beam Method or Iosipescu method	In-plane and interlaminar shear	**Compression**	*ASTM D5379*
Double notched shear test (DNS)	the in-plane shear	**Compression**	*ASTM D3846*
V-Notched Rail Shear test	In-plane and interlaminar shear	**Tension**	*ASTM D 7078-05*

Table 1: Setups for measuring interlaminar shear failure

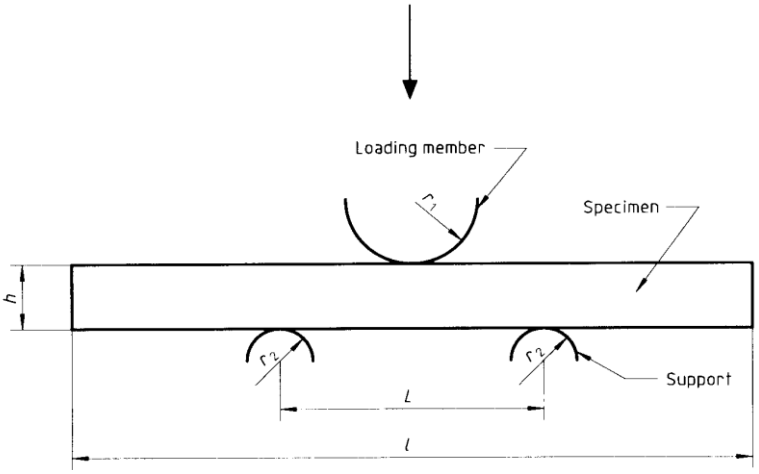

Figure 7 : 3points bending - Loading configuration (19)

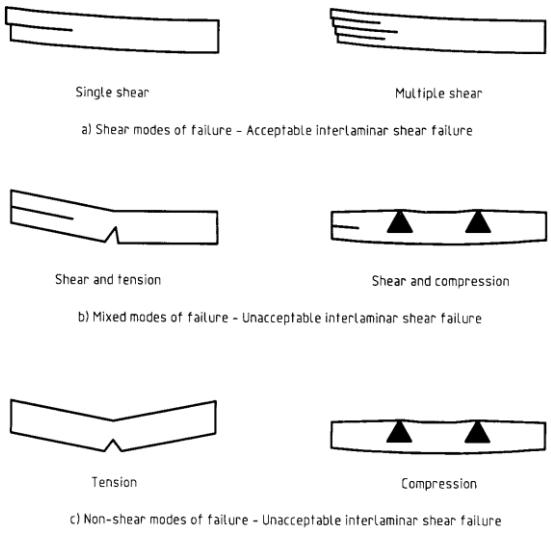

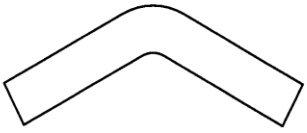

Figure 8 : Modes of failure (19)

The main asset of the short beam method is that the test setup is simple and does not require a specially designed test fixture to grip and load the specimen. Nevertheless, the test only provides an "apparent" shear strength using an assumed isotropic material stress distribution that also excludes the effect of other stresses due to the flexural loading and contact points. If one of the modes which are shown previously (Figure 8) occurs during the test, the failure could not be considered as an interlaminar shear failure and consequently the stress recorded will not correspond to the interlaminar shear strength. The setup has to be very accurately set without any play and the loading nose should load at exact distance between the two supports. The resulting data are depending on the sample geometry. This method has been very popular for a long time for characterizing the interlaminar shear failure resistance of fiber-reinforced composites. In the early 80”s, researchers started to wonder if this method was still suitable for new composite materials. Using, finite element scheme, they found that the stress distribution was not the one which was expected. Indeed, the load was mainly situated in the upper section of the beam near the nose. This configuration yields a stress concentration which can never be fully dissipated. (21)

In 1994, Ming Xie and Donald F, Adams showed with an analytical and an experimental study that the interlaminar shear strength depends on the thickness of the sample in the case of 3 and 4 point bending. Indeed, with low thickness, it was possible to reach greater shear stress. Moreover, the highest value of apparent shear stress was equidistant from the two supports and situated at middle thickness. (22) By the way, Ashbee in his book (23) advises to use the 3-points bending test only for thin composites of the same fiber volume fraction and only if the mode of failure is the good one. (Figure 8)

2.4.2. ±45° Tensile Test

Another method widely used in the field of composite materials is the Tensile Test of a ±45° Laminate. This method has two standards called ISO 14129 (24) and more recently ASTM D3518 (25). This test provides an indirect measure of the inplane shear stress-strain response in the fiber coordinate. A strain gage is placed in the coupon. This method is suitable only with fabric at ±45° to the specimen axis. (Figure 9) This method is popular because this is a simple tensile test which does need any special setup. The main constraint with this method is that the results are dependent on the number of layers or shearing interfaces in the sample. For example it is recommended keeping the number of shearing interfaces (surfaces) constant when the ply thickness varies. (26)

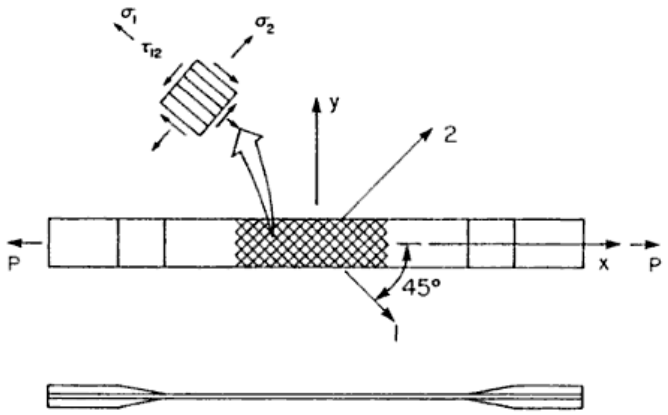

Figure 9 : Sample for ±45° Tensile Test - evaluation od shear stress response of unidirectional composites (27)

2.4.3. The V-Notched Beam Method or Iosipescu method

The V-Notched Beam Method or also called Iosipescu method was created in the middle of the 80s for measuring the interlaminar shear. This method has been standardized by the ASTM D5379 (28) in 1993. In this test, the sample is a rectangular flat strip with two V-notches (Figure 11) at the middle upper and lower surfaces. This sample is loaded in a special fixture (Figure 10). The notches influence the shear strain along the loading direction and make the distribution more uniform than without notches. This method is used for measuring in-plane and interlaminar shear properties. What makes this method so popular nowadays is because this method gives more real interlaminar shear failure results than with the short beam method. A special feature is needed and notches should be cut in the sample.

In 2000, Pettersson (29) evaluated experimentally with Digital Speckle Strain Mapping and Fractographic Analysis that the shear stress depends on the orientation of the fibers and is not homogenous and symmetric in the middle of the sample. Moreover, Hawong (30) in 2003 showed that the notch angle should be accurately made and an angle of 110° gives a better homogeneity compared to 90° for the shear stress especially in the center of the sample.

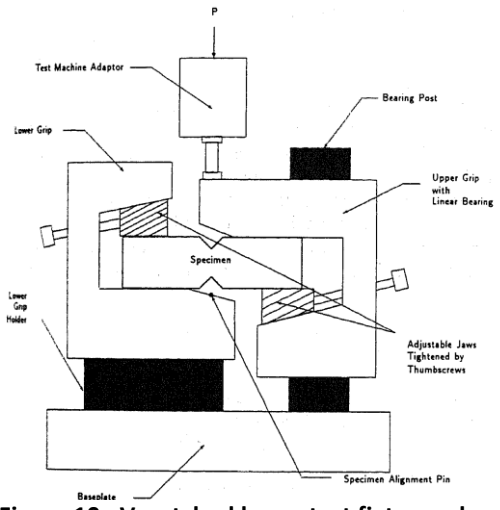

Figure 10 : V-notched beam test fixture schematic

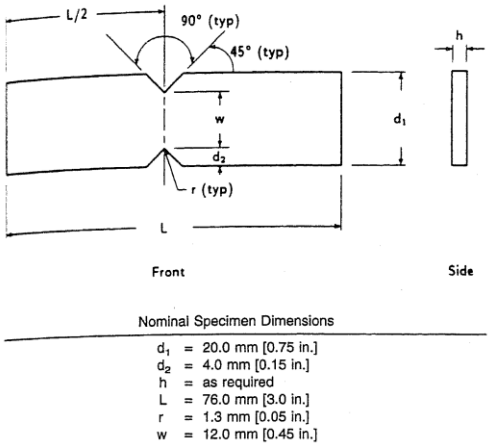

Figure 11 : V-Notched beam test coupon schematic

2.4.4. Double notched shear test (DNS)

The aim of this method is to measure the in-plane shear properties. The samples are rectangular bars with flat-bottomed notches staggered on the two opposite sides (Figure 12). When a tensile or a compressive force is applied a shear plane is created between the two notches. The severe stress concentration is created between the two notches makes the stress field inhomogeneous and consequently the results for the shear stress doubtful.

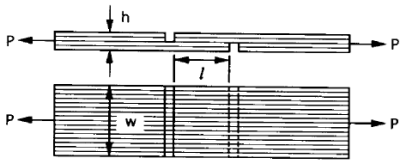

$$F_{31} \cong \frac{P}{wl}$$

$$\underline{\text{Note:}}\ \frac{2l}{h} < \frac{F_1}{F_{31}}$$

Figure 12 : Sample preparation for the double notched shear test (ASTM D3846)

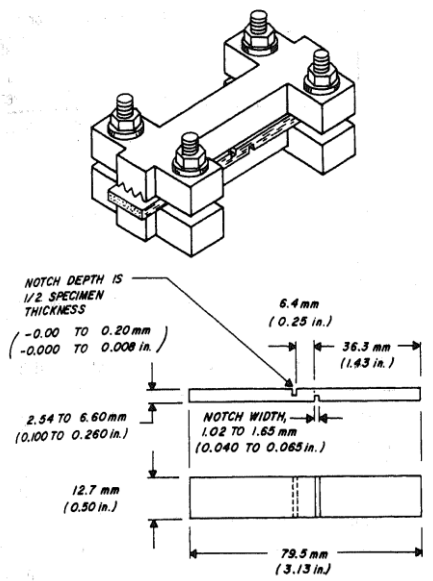

Figure 13: Specimen and loading jig for In-plane shear test

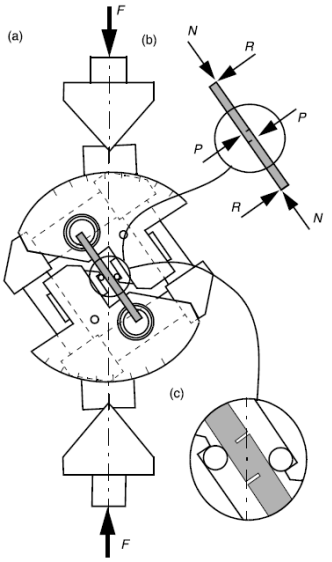

Fig. A1. The original compressive IDNS test setup (a) with external loading (F), (b) resulting specimen loading and (c) the rollers which apply the forces P in the test region.

Figure 14 : Inclined double notched shear test (IDNS).

In 1998, Neumaster and Palsson (31) improved this method using the same standard and the same samples but with an inclined setup (Figure 14). The method is called inclined double notched shear test (IDNS). The improvement in this method is that the appropriate combination of loads can minimize the stress concentrations between the notches while it produces a homogeneous state of true inter-laminar shear stress over the test region.

2.4.5. V-Notched Rail Shear test

Finally, the method mixing all the advantages of the previous methods is the V-Notched Rail Shear test which has been standardized by ASTM (32) in 2005. The V-Notched Rail Shear test has a relatively short history, but its use has grown rapidly. The test setup incorporates fixtures from the existing Iosipescu and the two rail shear tests. (33)

2.4.6. Conclusion

Interlaminar shear strength is a matrix dominant property and such improvement in interlaminar shear strength of fiber reinforced composites is mostly due to an improvement of the epoxy properties. This enhancement can be mainly achieved due to an increase of the interfacial area and due to good bonds between the particles and the matrix.

A lot of methods exist for measuring the interlaminar shear strength. Nevertheless, the short beam method is still widely used because this method is easy to perform and the setup is a normal 3-point bending for flexural strength where the span length has been reduced in order to induce interlaminar shear failure. Moreover the sample is a normal

rectangular sample. In some recent scientific papers, researchers characterized the interlaminar shear strength with the short beam method like Manfredi (34) studying in 2008, the addition of montmorionite in a glass fabrics/epoxy composite. In that case, shear strength was about 50MPa. Wishman (35) was successfully measuring the interlaminar shear failure of epoxy/fumed silica (7nm) with 37 and 50vol% of glass fabric using the same setup and the same standard.

2.5. Electrical breakdown

An electrical breakdown is a severe loss of the insulating properties of an electrical insulator. Electrical breakdown happens at a high voltage when the material changes its behavior from insulating material to conductive material. This can lead to a spark going around or through the insulator. This breakdown is very dangerous because it means that the insulator will lose its main function and let the electrical discharge passing through the material.

Nowadays, the new performance materials allow industrials to reduce the dimension of the insulating equipment while the heat density and the electrical current increase. The different types of breakdown are the electrical breakdown, the thermal breakdown and the electromechanical breakdown. The electrical breakdown occurs because the electric current starts to be unstable in the dielectric material or the electrical field reaches inadmissible proportion. The thermal breakdown is coming from the heating of the material by joule effect when an electric field is applied which can also produce relaxation phenomena. The increase of temperature can lead to the destruction of the dielectric. Finally, the electromechanical breakdown is coming because the material is subjected from electrical and mechanical stresses. For example, the attraction between the two electrodes can reduce the thickness of the sample by pressing it. It will follow a reduction of the dielectric strength.

The partial discharges are produced from local enhancements of the electrical field due to particles, local gaseous cavities, impurities in the material. Generally, three types of partial discharges can be encountered; internal discharges like those in electrical treeing, surface discharges and corona discharges. When the voltage reaches the value of the electrical breakdown of the gas (Pashen minimum), non-desirable reactions can appear like destruction of molecules, creation of radicals, local heating… Those phenomena will lead to the creation of prior path for the electrical current. The evolution of the electrical current in the material can be branched like a tree because of all those reactions. Knowing those facts, the material must be as perfect as possible, it means, free of gas-bubbles, cavities and impurities in order to obtain the best dielectrical properties. Surface discharges occur at the surface between two different medium with a different permittivity. Corona discharges are mainly coming from sharp metallic point in an electric field mostly in the high-voltage electrode. Partial discharges are a good indicator of the potential insulation failure of a material. It is possible to measure and localize

those partial discharges without damaging the material if the electric field is short in time and not too high.

At ABB corporate research center, for testing the electrical breakdown of a reinforced epoxy resin, two aluminum electrodes are embedded into the resin with a gap between the two electrodes. This mold is suitable only for measuring the breakdown strength of resin without glass fabrics. This setup is then tested inside a hermetic chamber filled with SF_6 gas. Another setup has been developed for testing a plate of glass mats reinforced epoxy. The plate is put between two electrodes dipped into silicon oil in order to insure a good insulation of the exterior medium and avoid flashovers. The problem with this method is that the silicon oil has to be changed after every test which makes this test polluting. One of the aims of this project is to develop a setup able to test a plate of glass fabric reinforced epoxy resin in a SF6 chamber. Imai (36) studied the impact of silica nanoparticles over the electrical breakdown strength in epoxy resin. This value was about 26% greater than the neat epoxy (at 50Hz with a rising speed of 0,6kV).

2.6. Dynamic Mechanical Analysis (DMA)

DMA gives information about mechanical properties of a specimen under oscillation (usually sinusoidal) as a function of time and temperature by putting it to a sinusoidal, oscillating force. The complex modulus E* is the ratio of the stress amplitude to the strain amplitude and represents the stiffness of the material. The complex modulus is composed of:

- The storage modulus E` (real part) which represents the stiffness of the **viscoelastic part** of the material. E` is proportional to the energy stored during a cycle. Used for determining the elastic properties of a material. In the glass transition region, the amorphous domains soften and the storage modulus drops in steps to a much lower value.
- The loss modulus E`` (Imaginary part) which is proportional to the energy dissipated during the load cycle and which cannot be recovered (heat…). Used for determining the **elastic viscous** of a material.

These characteristics depend on the frequency, the measuring condition and the history of the specimen.
The analytical parameters are:

- the amplitude of the deformation
- the stress
- the time displacement between deformation and stress

The phase angle δ is the phase between the dynamic stress and the dynamic strain in a viscoelastic material subjected to a sinusoidal movement. The loss factor tan δ is the ratio between the loss modulus to the storage modulus. Moreover, the Tg (temperature of glass

transition) of a material can be easily determined and is quite reproducible. This value represents the temperature when the loss modulus is at the maximum (Spectrum 1)

DMA is an equipment which can provide a rapid and convenient testing system for the determination of thermal mechanical properties of polymer or laminates as a function of the temperature, the time, the frequency using only a small amount of material. This fact is different for the mechanical properties which can vary depending on a lot of parameters. Some of them are the type loading and support clamps (3-point bending, single and dual cantilever), the machine (instrument design, machine compliance), the specimen alignment and the contact stresses. Knowing this fact, elastic moduli calculated with DMA, are often used only for screening material properties for quality control, research and development. Deng (37) compared the value of moduli from nanosilica reinforced epoxy obtained with DMA with different kind of loadings and supports and with a normal mechanical testing machine. His study showed that those methods were given similar results for the storage modulus but with a vertical shifting especially for the 3-points bending.

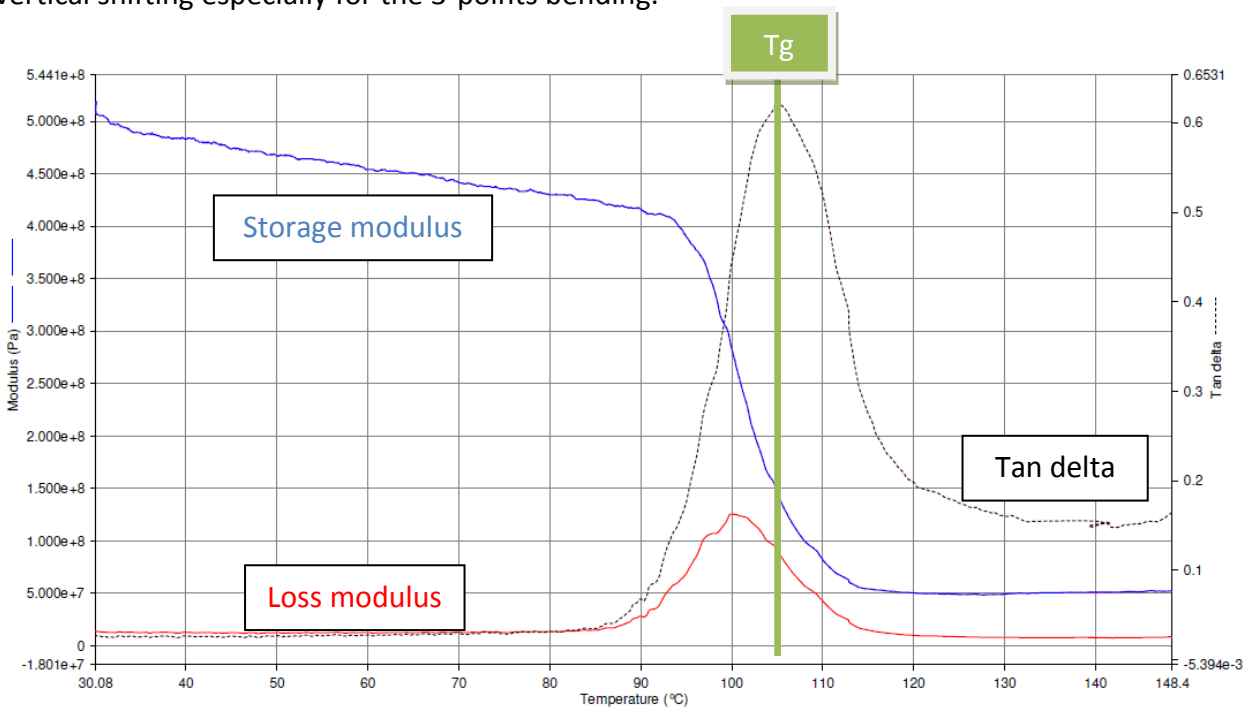

Spectrum 1 : Graph representing, the storage modulus (blue curve), the loss modulus (red curve) and the tan delta (black curve) – nanocomposite reinforced epoxy

3. MATERIALS

3.1. CY225/HY925: Reference

In this project, the epoxy resin used as a reference is the ARALDIT CY225 based on bisphenol-A with epichlorohydrin (DGEBA) and the hardener is ARALDIT HY925, an anhydride based on a preaccelerated methyltetrahydrophthalic anhydre (MTHPA) both supplied by

Huntsman, Switzerland. With this couple, the blend is degassed and preheated at 65°C for impregnation, and cured for 8 hours at 140°C. The main assets of this epoxy resin are a high glass transition temperature which gives high mechanical and electrical properties at elevated temperature, a good thermal shock resistance and excellent toughness. The main applications of this epoxy resin are not only indoor electrical insulators for medium and high voltage, such as switch and apparatus component but also the encapsulation of metals parts and for all the application with a long term stresses up to service temperature of 85°C (38).

Component	Trade name	Supplier	Chemical name	Parts per hundred resin (phr)	EEW (Epoxy equivalent weight) (g/mol)
Resin	Araldite® CY 225	Huntsman, Switzerland	bisphenol-A with epichlorohydrin (DGEBA)	100	192
Hardener	HY 925	Huntsman, Switzerland	Preaccelerated methyltetrahydrophthalic anhydre (MTHPA) (M:166g/mol)	80	

Table 2 : System used as a reference and for masterbatch dilution

3.2. Particles

Ceramic particles are evaluated for the improvement of thermal conductivity of glass reinforced epoxy.

3.2.1. Particle 1 (P1 - 700nm)

Particles 1 are submicron particles with an average diameter of 700nm, supplied in powder (Figure 15). The particles are mixed at 65°C with the reference epoxy a various concentrations under vacuum (Table 2). The samples are cured at 140°C for 8hours.

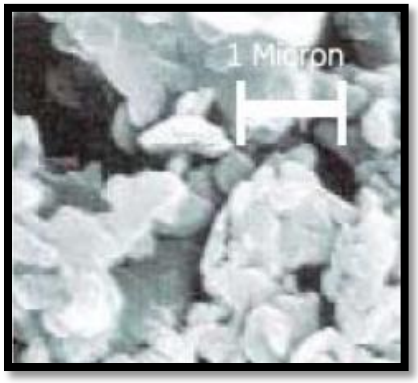

Figure 15: Particles P1 - 10000x

3.2.2. *Particle 2 (P2 - 70nm)*

Particles 2 have an average diameter of 70nm are supplied in a masterbatch with 40wt% of particles is dispersed in EPON 828 (Table 3). The masterbatch is diluted with the reference epoxy (Table 2); it is mixed at 65° at various concentrations under vacuum. The samples are cured at 140°C for 8hours.

Component	Trade name	Supplier	Chemical name	Parts per hundred resin (phr)	EEW (Epoxy equivalent weight) (g/mol)
Resin (Masterbatch)	EPON® 828	Shell Chemicals	bisphenol-A with epichlorohydrin (DGEBA)	100	185 – 192
Hardener	HY 925	Huntsman, Switzerland	preaccelerated methyltetrahydrophthalic anhydre (MTHPA)	81,6	

Table 3 : System for masterbatches Nanosperse, LLC, USA containing 40wt% of P2 particles (70nm) or P5

3.2.3. *Particle 3 (P3 – 100nm)*

P3 particles with an average diameter of 100nm in modified bisphenol A is supplied in a masterbatch. The 49,8wt% masterbatch is cured with 81,3 phr HY925 (Table 4). The resin is mixed at 65°C under vacuum and cured at 140°C for 8hours.

Component	Trade name	Supplier	Chemical name	Parts per hundred resin (phr)	EEW (Epoxy equivalent weight) (g/mol)
Resin (Masterbatch)	(trade secret)		bisphenol-A based modified epoxy resin	100	189
Hardener	HY 925	Huntsman, Switzerland	preaccelerated methyltetrahydrophthalic anhydre (MTHPA)	81,3	

Table 4 : System for masterbatch containing 40wt% of P3 particles (100nm)

3.2.4. *Particle 4 (P4 – 45nm)*

P4 particles with an average diameter of 45nm are supplied in a masterbatch with 22,5wt% of particles dispersed in ARALDIT F (Huntsman, Switzerland), cured for 6 hours at 80°C and 10 hours at 130°C. The blend is preheated at 60°C. (Table 5)

Component	Trade name	Supplier	Chemical name	Parts per hundred resin (phr)	EEW (Epoxy equivalent weight) (g/mol)
Resin	ARALDIT® F	Huntsman, Switzerland	bisphenol-A with epichlorohydrin (DGEBA)	100	187 – 192
Hardener	HY 905	Huntsman, Switzerland	1,2-Cyclohexanedicarboxylic Anhydride (M: 154,17g/mol)	100	
Accelerator	DY 062	Huntsman, Switzerland	Tertiary amine	0,8	

Table 5 : System with masterbatch containing 22,5wt% of P4 particles (45nm)

3.2.5. Particle 5 (P5 – 15/30nm)

P5 particles with an average diameter of 15 to 30nm (Figure 16) are supplied in a masterbatch with 40wt% of particles dispersed in EPON 828 (Table 3). The masterbatch is diluted with the reference epoxy; it is mixed at 65° at various concentrations under vacuum. The samples are cured at 140°C for 8hours.

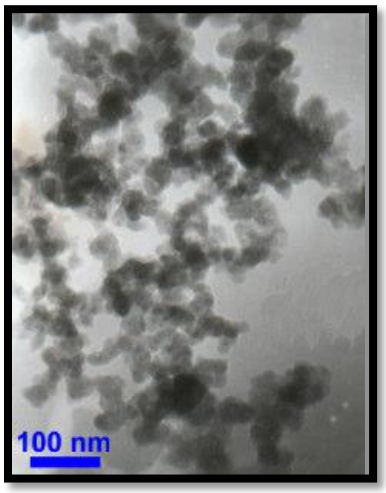

Figure 16: Particles P5 (15 - 30 nm)

3.3. Glass fabric

3.3.1. Glass fabric

For reinforcement, two types of glass fabrics supplied in rolls by Swisscomposites, Switzerland have been selected in this project (Table 6).

- **ATLAS 1/7** fabric has the same number of fibers in both X and Y directions. Atlas 1/7 means that the weave pattern has a tow travelling in the X direction which lies over one bundle and under seven bundles of fibers. This type of weaving is atlas (Figure 17).

- **UD KÖPER 1/3** fabric is a Unidirectional mat which means that the main number of fibers travels in one direction. Fabrics in the cross direction are holding the fibers together. Köper 1/3 means that the weave pattern has a tow travelling in the x direction which lies over one bundle and under three bundles of fibers. The unidirectional fabric is used to obtain the maximum reinforcement in one direction at the expense of the other (Table 6). The type of weaving is twill (Figure 17) which is characteristical of diagonal parallel ribs.

3.3.2. Cleaned glass fabrics

These fabrics have been washed and supplied by TESSA AG.

- **Mehrlagengewebe** is a multi-layer glass fabric (ML) with a thickness of 0,40mm per layer. No more information has been distributed by the supplier about the weave pattern (Figure 18). The X-direction is the weft yarn with E-glass Continuous 9-136 with 11 threads and the Y-direction is along the warn yarn with E-glass Continuous 9-68 with 20 threads (Table 6).

- **ATLAS 1/7**. This fabric is similar to the previous ATLAS 1/7 (same weave pattern) except for the thickness (0,24) and the final treatment.

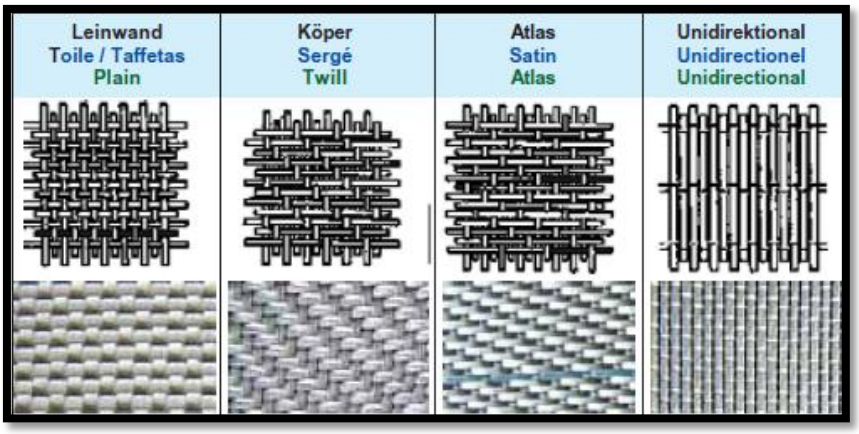

Figure 17 : Glass fabrics used in this project for reinforcement (39)

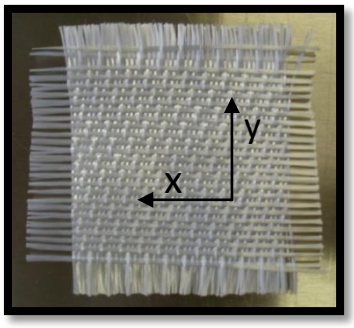

Figure 18: ML Mehrlagengewebe glass fabric, Y-direction is along the warp yarn and X-direction is along the weft yarn

Weave Pattern	Warp Yarn / Weft Yarn	Tread count Warp/weft (thread/cm)	Thickness (mm)	Weight (g/m²)	Supplier
ATLAS 1/7	EC 9-34X2/EC 9-34X2	22/21	0,40	300	Suter Swiss composite
UD-KÖPER 1/3	EC 9-136/ EC 7-22	19/12	0,28	286	Suter Swiss composite
ATLAS 1/7 (cleaned)	EC 9-68/EC 9-68	22,9/21,1	0.24	300	Tessa AG
Mehrlagengewebe ML (cleaned)	EC 9-68/ EC 9-136	20/11,75	0.38	300	Tessa AG

Table 6 : Glass fabrics used as reinforcement

Example: Atlas 1/7 – EC 9-34X2/EC 9-34X2
E = E-Glass
C = Fiber of infinite filaments (Continuous)
9 = Diameter of the filaments (µm)
34 = tex (number of filaments)
The warp is the lengthwise threads attached to the loom before weaving. Then the weft is woven back and forth through the warp to make the fabric.

3.4. Room temperature curing epoxy resin (RT epoxy)

RT epoxy (Table 7) is used for filling bored holes in the electrical breakdown test sample. The curing is approximately 24h at room temperature and the gel time is 60min at 25°C. The main properties of this RT epoxy are a good heat resistance, a resistance to chemical degradation, a low viscosity and a curing at room temperature. The main industrial applications are the encapsulation or potting of low voltage components.

Component	Trade name	Supplier	Chemical name	Parts per hundred resin (phr)	EEW (Epoxy equivalent weight) (g/mol)
Resin	Araldite DBF	Huntsman, Switzerland	Epoxy resin modified by the addition of a plasticizer	100	235
hardener	HY 956 EN	Huntsman, Switzerland	Polyamine	20	

Table 7 : Room temperature curing epoxy resin (based on Araldite DBF)

.

4. EXPERIMENTAL: PROCESSING AND CHARACTERIZATION

4.1. Processing

4.1.1. Casting of plates

Casting is used to produce plates of neat or filled epoxy; a mold of polished plates covered with release agent (QZ 013, Huntsman, Switzerland) is assembled and preheated at 65°C. The resin system is prepared and mixed under vacuum (7 mbars); the mixture is poured into the mold. The resin is degassed at 65°C once more in the mold and cured according to the prescribed schedule.

4.1.2. Impregnation of laminates

RTM (Resin transfer molding) and VARTM (Vacuum assisted resin transfer molding) are processes used to produce impregnated fabric composite. Pressure is used to force resin into the mold by RTM while the mold is filled with vacuum in VARTM.

The RTM/VARTM setup is composed of a vacuum trap, a pressure tank, plastic tubing, a vacuum pump and a source of pressurized air (Figure 19). The flow rate is measured with a scale (flow rate between 50 and 120g/min) and controlled with clamps. The mold is cleaned, polished and coated with release agent (QZ 013, Huntsman, Switzerland) and the precut E-glass fabrics are placed inside (Figure 20); rubber seals are used. The completed mold and pressure tank are preheated at 65°C. The resin is prepared as described previously.

In RTM, the resin is injected with pressurized air approximately 0.5 bars depending on the blend with a flow rate of 50g/min. This process is used with a mold of dimensions 20 x 21cm. The mold is filled, vacuum is applied slowly to 1 mbars in approximately 5 min and held for at least 5 min) to remove the air bubbles. An overpressure of 5 bars is applied and held for 3-4 min to improve the impregnation of the resins through the fabrics. The inlet and outlet tubes are clamped and the mold is put in an oven for curing.

In VARTM, the resin is injected by applying vacuum slowly. A valve is connected between the pressure vessel and the mold to regulate the flow of resin. This process is used with a mold of dimensions 40 x 43cm. Vacuum is applied only to the mold in order to remove air from the mold and the fabrics to 1 mbars in 10-15 min and it is held for 5-10 min. Then, the valve is opened and resin is allowed to flow from the pressure vessel to the mold at a rate of 40 – 150g/min. The mold is filled, the valve is closed and vacuum is still applied in order to remove the remaining air bubbles for 5 to 15min. An overpressure of 3 to 5 bars is applied and held for 3-4 min to improve the impregnation of the resins through the fabrics. The inlet and outlet tubes are clamped and the mold is put in an oven for curing.

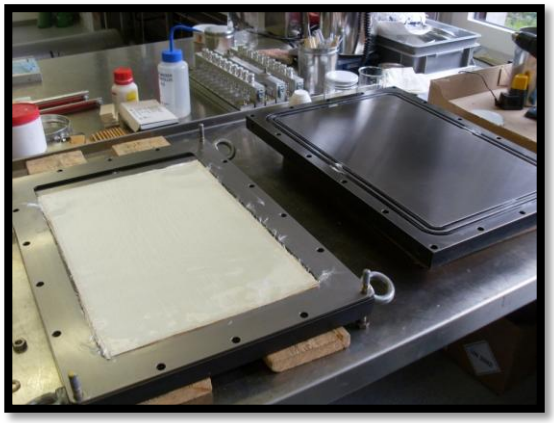

Figure 19 : Mold for preparing laminates of glass fabrics reinforced epoxy resin (on the left: top of the mold with the glass fabrics, on the right: bottom of the mold)

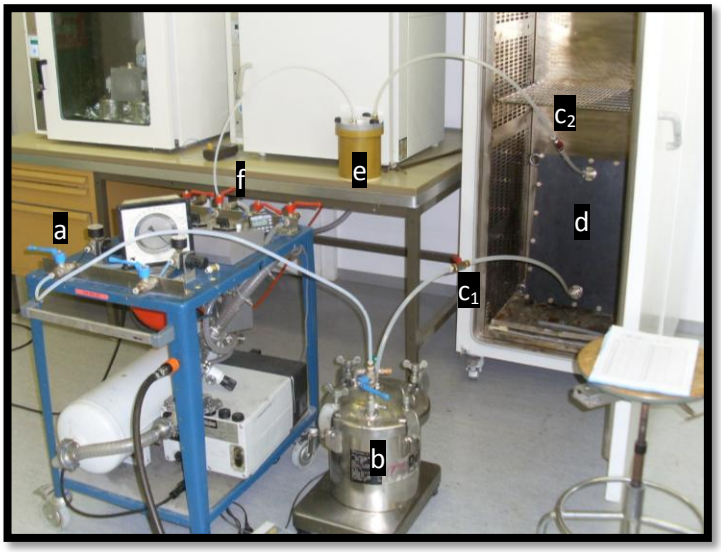

Figure 20 : Setup for impregnation of a laminate 30x44cm a:Air pressurized tube, b:Pressure tank containing the blend, c: valves, d: mold, e: vacuum trap, f: inlet for vacuum

4.1.3. Wet lay

Resin is applied over glass fabrics of 21x20cm dimension layer by layer by hand (Figure 21a). The resin is prepared as described previously. The resin is spread over the fabric with a spatula. Air bubbles are removed with the spatula. Once the fabrics are impregnated, the plate is put into a press with a pressure at 20 Bars and an initial temperature of 70°C for 15 min and then cured at 140°C for 8 hours (Figure 21b). The thickness of the plate is controlled with spacers. Plates of 60vol% of fibers are prepared by this method.

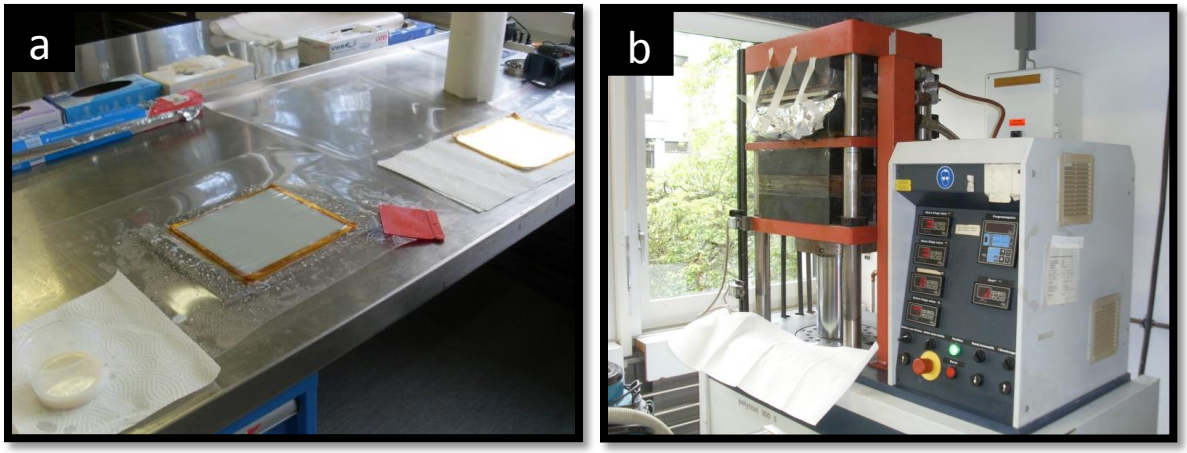

Figure 21 : a: impregnation of the fabrics with a spatula, b: hydraulic press for making wet lay plates

4.1.4. Electrical strength samples

A two half mold is used to prepare samples of laminates for breakdown strength measurements in SF_6 gas. The mold is covered with released agent and a 120x120x4mm cast or laminate test plate is placed between the two halves (Figure 22). After assembly, the mold and the plate are preheated at 65°C and resin is injected by VARTM. The sample is ground, voids are filled with epoxy and the surfaces are painted with silver (Figure 23).

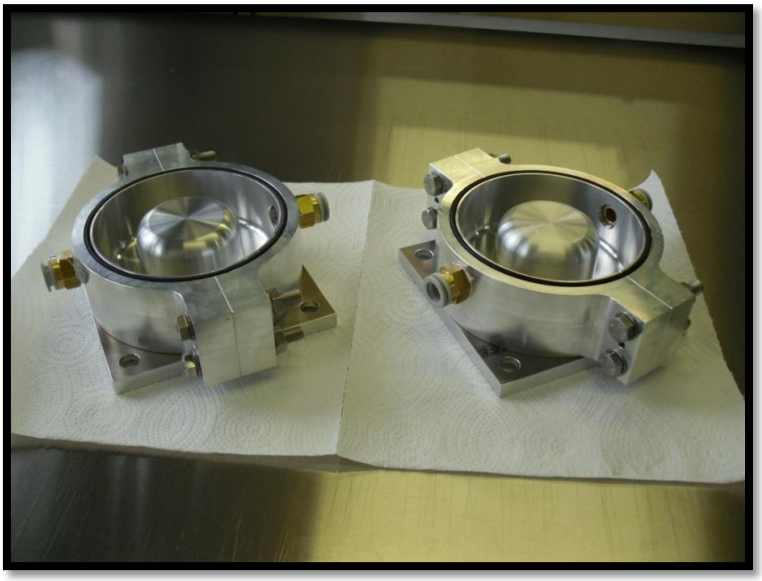

Figure 22 : Mold for injection of sample for electrical breakdown tests

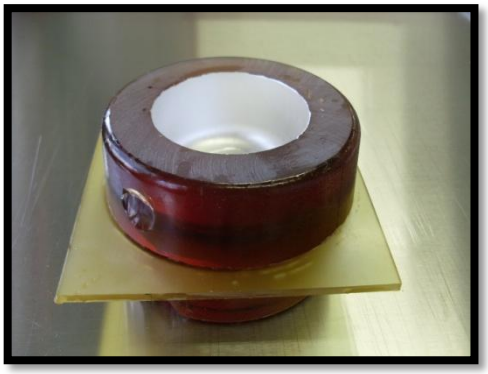

Figure 23 : Sample for electrical breakdown test with the protective walls and painted with silver

4.2. Characterization

4.2.1. Viscosity

Viscosity measurements are made with a C-VOR rehometer from Bohlin instruments. The **viscosity** is measured with two parallel plates (40 mm diameter) with a gap distance of 500 µm and a constant shear rate of 10 s^{-1}. over a temperature range of 30 to 90°C with a heating rate of 3°C/min.

4.2.2. Reaction enthalpy and glass transition temperature, Tg

The **reaction enthalpy** of uncured samples is measured with a Perkin Elmer DSC 7. 8 to 10 mg are placed in an aluminum pan and heated from 30°C to 275°C with a heating rate of 10°C/min; the enthalpy is determined. The **Tg** of cured samples is measured with Perkin Elmer DSC 1. 15 to 35 mg are placed in an aluminum pan and heated twice from 30 to 200°C with a heating rate of 10°C/min; the Tg is determined from the second heat scan. A baseline is subtracted from all measurements.

4.2.3. Degradation temperature, Td and the residue weight

Td and **the residue content** are measured with a Q500 TGA (*Thermal Gravimetric Analysis)* from TA instruments. The samples are heated from 30°C to 800°C with a heating rate of 10°C/min. The Td is taken at a weight loss of 1wt% and 5wt%. The weight of particles in a sample is calculated from the residue weight at 800°C.

4.2.4. Thermal conductivity λ

Circular samples of diameter 50,8mm and a thickness of 4mm are measured with an Anter Unitherm Model 2022 according to ASTM E1530 test method. The **thermal conductivity** is measured at 40°C, 60°C, 80°C and 100°C.

4.2.5. Microscopy

Samples are observed by **optical microscopy** (OM) with a *Karl Zeiss microscope* and by **scanning electron microscopy** (SEM) with a VEGA XMU from *Tescan USA Inc*. Samples are embedded into an epoxy resin, ground, polished and coated by sputtering with either 5nm of gold or carbon for SEM.

4.2.6. Storage and loss modulus

The **storage modulus, loss modulus and tangent** are measured using a Perkin Elmer TMA7/DMA7e. The moduli and tangent are measured for matrix materials only. The sample dimensions are 19mm x 10mm x 1mm. The measurements are performed with a heating rate of 5°C/min, with a forced oscillation frequency of 1Hz and a static and dynamic force of 110mN and 100mN, respectively. Figure 24 shows the 3-points bending setup where the sample is kept free at the 3 points.

Figure 24 : Storage and loss modulus measurements, for 3-points bending

4.2.7. Thermal expansion coefficient α (CTE)

The **thermal expansion coefficient** is measured using a Perkin Elmer TMA7/DMA7e. In TMA mode, matrix and laminate samples with dimensions of the 6mm x 6mm x 4mm are

measured with a heating rate of 2°C/min from -10 to 160°C, a static force of 100mN and dynamic force of 110mN. The coefficient of thermal expansion is measured during the second heating cycle.

4.2.8. Relative permittivity and dissipation loss factor

The **relative permittivity** ε_r and the **dielectric tangent factor** tangent δ are measured from 1 to 10^6 Hz at 40°C, 60°C, 80°C, 100°C, 120°C and 140°C using a novocontrol according to CEI IEC 250. Samples dimensions are 38mm x 38mm with thickness 1 mm for the matrix and 4 mm for laminates. The samples are placed between two gold electrodes of 20mm diameter under a voltage of 5V. The plates are washed and held in a dessicator for 24 hours before measuring.

4.2.9. Fiber volume percent

The **fiber volume percent** is calculated according to the standard ASTM D2584-02, samples of 25mm x 25mm x 4mm are weighted with a micro-scale (METLER AE240). The square samples are burned in an oven up to 600°C with a heating rate of 10°C/min and held at for 4 hours. The residue is weighted and the fiber volume percent is calculated.

4.2.10. Density

The **density** is measured with a Mettler ME-40290 installed on a Mettler AE 240 scale (Figure 25). Samples of 25mm x 25mm x 4mm are cleaned, dried and weighed in air and in water. Using Equation 1 , the density of the sample is determined:

$$\rho_1 = \frac{A}{P} \cdot \rho_0 \left[g / cm^3 \right]$$

Equation 1

Where ρ1 is the density of the sample, ρ0 is the density of water (0, 997g/cm3 at 25°C), A is the weight of the sample in air and P is the weight of the sample in water.

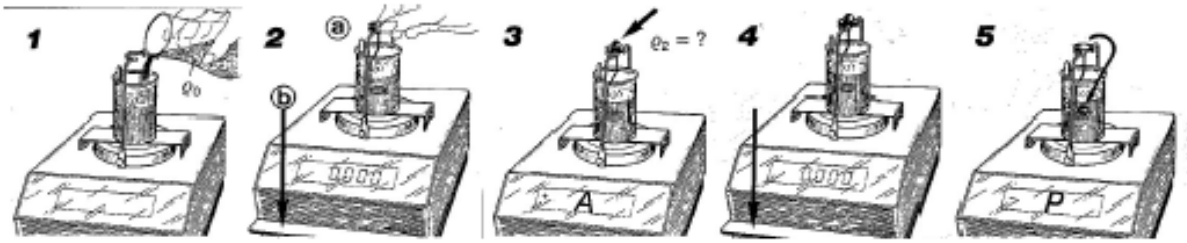

Figure 25 : Procedure for measuring the density: 1: Beaker glass is filled with distilled water, 2: weighting scale is placed and the scale is tared, 3: the sample is weighed in air, 4: The scale is tared, 5: The sample is weighted in water

4.2.11. Flexural and interlaminar shear strength

Flexural properties and **interlaminar shear strength** are measured with a Zwick Roell 100 and a 3-points bending setup (Figure 26) according to the standard ISO 14125, and ISO 14130 and ASTM D2344, respectively. Flexural samples of the matrix have dimensions of 80x10x4mm and are measured with a strain rate of 1,7mm/min. Flexural samples of the laminates have dimensions of 80x15x4mm and are measured with a strain rate of 1,7mm/min (Table 8). Flexural measurements are performed with a load cell of 5kN maximum and calculated using the equation 2. Interlaminar shear strength is measured by two standards; the parameters are described in Table 9 and Figure 26. Shear measurements are performed with a load cell of 100kN at a strain rate of 1mm/min and calculated using the equation 3. All measurements are performed at room temperature.

Test	Standard	Dimensions (Length x Width x thickness)	Span (mm)	Loading members Radius (r1 and r2)	Speed (mm/min)
Flexural Properties	ISO 14125	80 x 10 x 4 (Matrix)	64	5mm	1,7
		80 x 15 x 4 (Reinforced with 30vol% E-Glass)	64	5mm	1,7

Table 8 : Parameters used for flexural properties measurements

Test	Standard	Dimensions (Length x Width x thickness)	Span (mm)	Loading members Radius (r1 and r2)	Speed (mm/min)
Interlaminar shear strenght	ISO 14130	18 x 6 x 3	15	5mm and 2mm	1
Interlaminar shear strenght	ASTM D2344	30 x 15 x 3	12	6mm and 3mm	1

Table 9 : Parameters used for interlaminar shear measurements

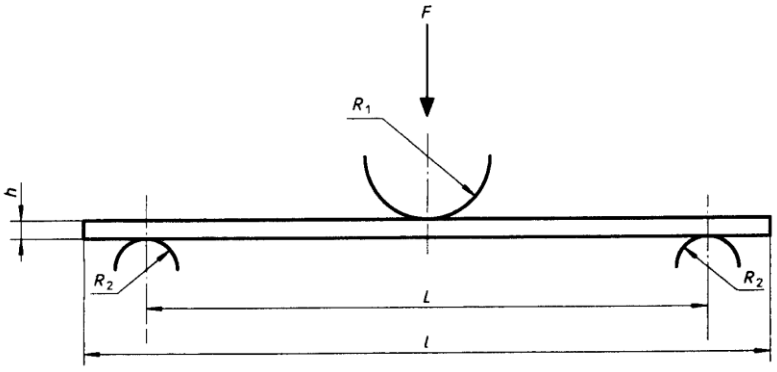

Figure 26 : Schema of the setup for measuring flexural strenght and interlaminar shear strenght (Source: Standard Iso 14130) – h:thickness of the sample, R1: radius of the loading member, R2: Radius of the support members, L: Span (length between the two supports).

$\textbf{Equation 2 : } \sigma_f = \frac{3FL}{2bh^2}$	$\textbf{Equation 3 : } \tau_M = \frac{3F}{4bh}$
Flexural strength in MPa according to the standard ISO 14125 F is the load (N), L is the span (mm), h us the thickness of the specimen (mm) and b is the width of the specimen (mm)	**Apparent interlaminar shear strength in MPa** *According to the standard ISO 14130 and ASTM D2344 F is the maximum load observed (N), h us the thickness of the specimen (mm) and b is the width of the specimen (mm)*

4.2.12. Partial Discharges (PD)

The partial discharge measurements were carried out using a PD instruments from Lemke Diagnostic, Germany. The standard used for these tests is IEC 60270 (40). The sample should be free of partial discharges at 20kV. Germany. Before every measurement of electrical breakdown strength, the sample is placed between two electrodes and the number of partial discharges is measured in pC (Pico-coulomb) at a certain voltage (in kV) to know if a sample is suitable or not for further electrical measurements (Figure 27).

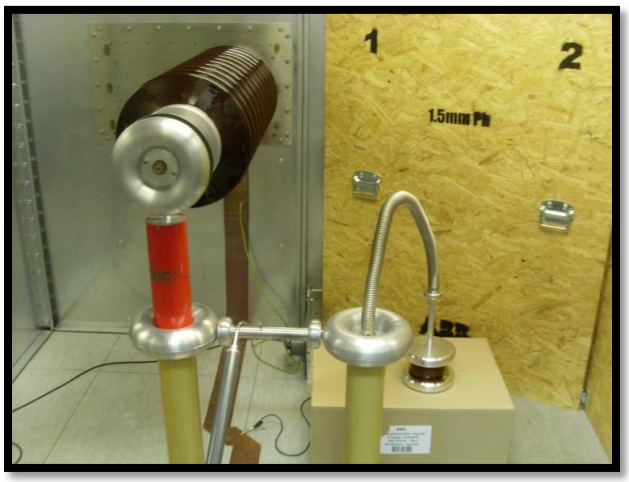

Figure 27 : Setup for Partial discharges measurements (PD)

4.2.13. Electrical breakdown strength

The electrical strength is measured in a sealed chamber filled with 5 bars of SF_6 according to IEC 60243-1 (Figure 28). In a preliminary setup a plate with dimensions 120mm x 120mm x 1mm is placed between two spherical electrodes with a diameter of 38mm (Figure 29a). In a second setup (Figure 29a), a plate with a thickness of 4mm prepared as described in a previous section is used (section page 25, Figure 23). The voltage is increased stepwise by 1V every 60 seconds with both test setups. The breakdown strength is determined from the peak to peak distance divided by square root of 2. The electrical breakdown strength represents the ultimate value of the current when the breakdown occurs.

Figure 28 : Chamber for electrical breakdown testing

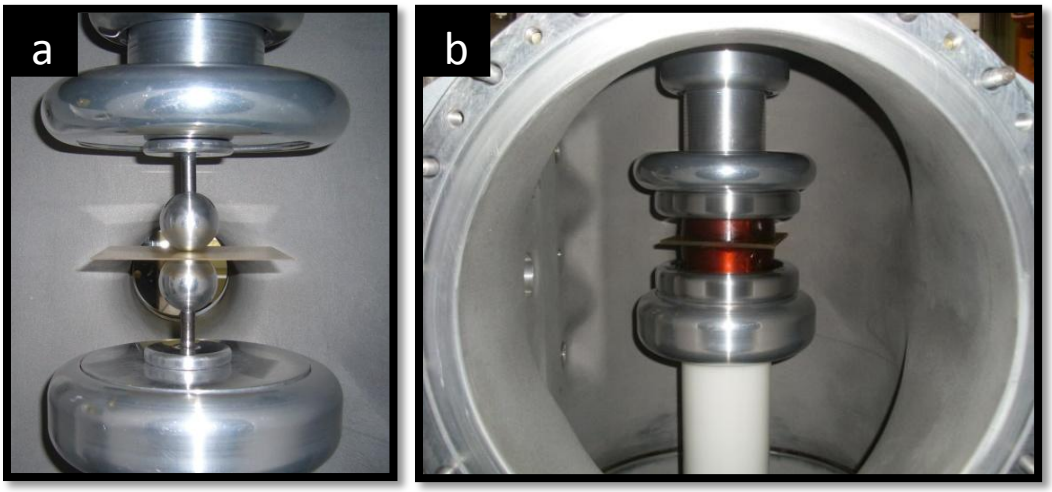

Figure 29 : a: Preliminary setup for electrical breakdown with spherical electrodes - b: Sample with the second setup in the GIS (Gas insulated Switchgear)

5. RESULTS AND DISCUSSIONS

5.1. REFERENCE CY225/ 80 phr HY925

CY 225 with 80 phr HY 925 is used as a reference. The resin is employed for dispersion of particles and dilution of prepared masterbatches. This epoxy is flexible and ductile which allows for easy handling for casting and molding. The use of a reference allows for the determination of the impact of particles on the thermal, mechanical and dielectric properties of the resin. Processing, thermal conductivity, electrical and flexural properties are tabulated (Table 10).

Reference	ΔH [J/g]	Td °C 99% 95%	ΔH [J/g]	$T_{reac.}$ [°C]	Tg [°C]	η [Pa*s] (@65°C)	λ [W/m*K] (40-100°C	ε_r (40°C ,50Hz)	Tanδ (40°C, 50Hz)	E_f [N/ m^2]	$\sigma_{f,max}$ [N/m²]	α 10^{-6}/°C
CY225/ 80phr HY925	300,9	312,6 360,5	300, 9	169, 5	124, 5	0,094	0,19	3,47	2,92E-03	3035	114,3	62,09

Table 10: CY225/ 80phr HY 925 reference resin system: processing, thermal, mechanical and dielectrical properties (1)

DMA measurements are performed to obtain information about the storage modulus, the loss modulus and the glass transition temperature; Tg. Samples with thickness of 1mm are tested by 3 points bending measurement. DMA measurements with 3-points bending were successfully carried out with all the materials. The appropriate tests parameters were determined from experiment to be a static force of 110mN, a dynamic force of 100mN, a frequency of 1Hz and a heat rate of 5°C/min. Differing results were obtained for the reference epoxy (CY225/80phr HY925).

A spectrum is obtained using the 3points bending set-up (Spectrum 2). The storage and loss modulus, and Tg measured with 3 points bending setup for reference material is given in (Table 11) In 3points bending mode (Spectrum 2), the storage modulus at 40°C is 907MPa and the maximum of loss modulus is 227MPa at 92°C. The Tg (tan δ) is found at 99°C which is lower than the Tg measured with dual cantilever and DSC (1).

3-points bending	Storage modulus			Loss modulus	Maximum loss modulus	Tg (tan δ peak)
Temperature	40°C	80°C	140°C	40°C	92°C	99°C
MPa	907	704	21	44	227	

Table 11: Dynamical mechanical properties measured with dual cantilever and 3-points bending test setups of reference CY225/ 80phr HY925 (sample thickness of 1mm)

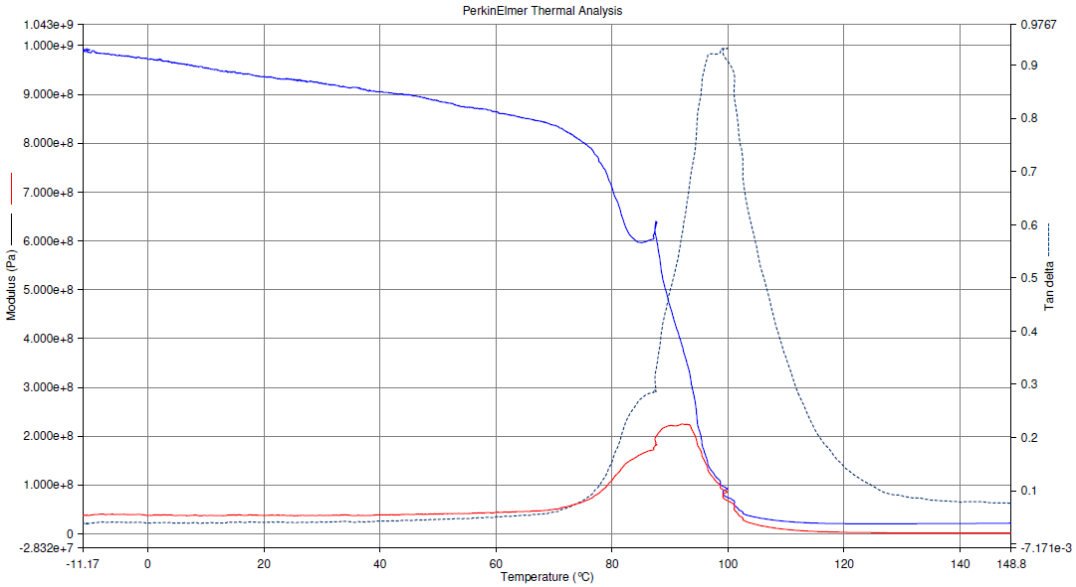

Spectrum 2 : Dynamical mechanical properties for 3points bending of a plate with a thickness of 1mm of the neat resin - F:100mN

5.2. Laminates: E-glass fibers

Glass fibers are used to reinforce epoxy; previously, four different E-glass fabrics (9 µm fibre diameter) were evaluated, including: Leinwand (plain weave), Köper (twill weave), Atlas (atlas weave) and unidirectional (unidirectional weave). The flexural properties in the warp direction and the thermal conductivity of the laminates were measured and a fiber volume of 30vol% was chosen for all the laminates. Also, it was previously observed that an impregnation with 50vol% fiber led to filtration of resin. The atlas weave pattern (Isotropic - same number of fabric in both directions) is selected for further experiments based on previous mechanical results. (1).

Two types of clean glass fabrics are evaluated: an atlas 1/7 weave pattern with a thickness 0.24mm and a multilayer (ML) weave pattern with a thickness of 0,38mm. ML fabric is evaluated for impregnation to determine if the lack of sizing would affect the laminate. Clean fabrics are used in all further laminate preparation: it has been shown previously that the impurities on the fiber surface or in the weave provide a path for electrical breakdown to occur (41). The fabrics are observed with an optical microscope (Figure 30 and Figure 31). The clean glass fabric shows less contamination than the unwashed material although the clean fabric has some impurities on the surface. A difference between the fabrics is observed during the cutting; the two clean fabrics unravel and electrostatically charge easily. Fabric rolls were stored in a clean environment and wrapped carefully to avoid contamination in storage. The fabric is cut on a clean table with clean tools to avoid the impurities.

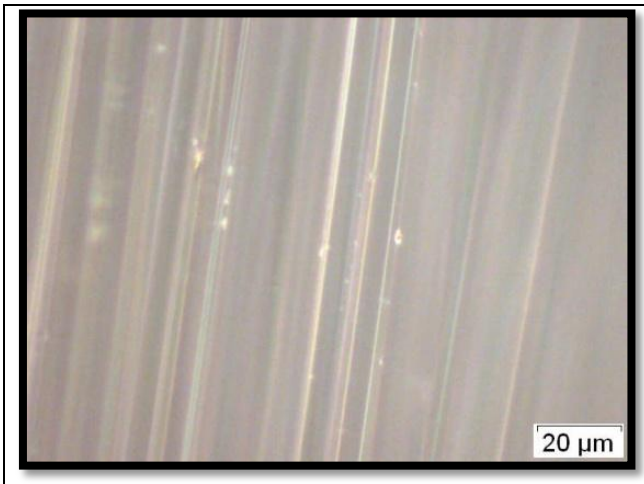

Figure 30 :Optical micrograph of the surface of an unwashed E-glass fabric with UD Köper 1/3 weave pattern (OM - x500)

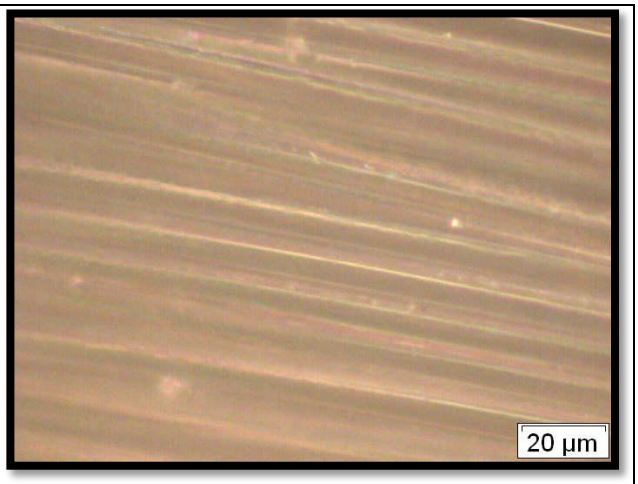

Figure 31 : Optical micrograph of the surface of an unwashed E-glass fabric with Atlas 1/7 weave pattern (OM - x500)

Thermal expansion is a very important parameter in the case of molding pieces and insulator. The thermal expansion coefficient describes how the size a piece changes with a change the temperature. The addition of ceramic particles and glass fabrics affect this coefficient. For making the electric breakdown samples, two solutions are possible, the walls and the plates are made from the same material or the plate is made from the material which has to be tested and the wall is made from the epoxy reference without fillers. The last case will be the more economical because it will save expensive material. In order to avoid cracks after injection, the expansion coefficients of the two materials must be quite similar. The thermal expansion in theory of E-glass is $4{,}9.10^{-6}$/°C **(42)**. The thermal expansion of epoxy resin with 30vol% non-washed and clean Atlas 1/7 glass fabric is respectively 66,09 10-6/°C and 44,34 10-6/°C which is an augmentation of 6,31% and a reduction of 28,6% compared to the matrix reference (Table 12).

Reference CY225/ 80 phr HY925	Thermal Expansion coefficient 10^{-6}/°C
Matrix	62,09
Laminate with 30vol% unwash Atlas 1/7	66,01
Laminate with 30vol% clean Atlas 1/7	44,34

Table 12: Thermal expansion coefficient of the reference epoxy resins

The dielectric dissipation of E-glass fibers is a little bit higher than the typical epoxy (43). The dielectric permittivity of the laminates with the reference epoxy and 30vol% clean glass fabric is measured at 50Hz, ε_r is 4,43 for ML cleaned fabric and 4,28 for clean Atlas 1/7 glass fabric at 40°C (Table 13). The dielectric dissipation factor is $3{,}06E^{-3}$ for ML clean fabrics and at 40°C and $2{,}36E^{-3}$ for Atlas 1/7 clean fabric; Tan δ is measured at 50Hz. ML clean glass fabrics

exhibit an increase of the dielectric permittivity of approximately 3,5% and of 29,7% the dielectric dissipation factor of compared to atlas 1/7.

The relative permittivity of a material describes the relationship between AC signal's transmission speed and the dielectric's material capacitance relative to the vacuum. The dissipation factor or loss tangent is the ratio of the energy dissipated such as heat to the energy stored into the material. A good dielectric means that the all the signal pass through the dielectric without being absorbed in the material. A material with a large dissipation factor subjected to high power signals could develop an important amount of heat and even goes up in flames.

The addition of 30vol% clean glass fabric increases the permittivity of 27,7% for ML and of 23,3% for atlas 1/7 and the dielectric dissipation factor of 4,8% for ML but decrease the Tan δ of 19% for atlas 1/7 at 40°C. The augmentation of permittivity comes from the addition of 30vol% glass fibers and from the new interfaces matrix/fibers in the material. The laminates with clean ATLAS glass fabric shows an enhancement of the dissipation loss factor because the use of clean fabric, where oil and dust have been removed, makes the interface better between the fibers and the matrix.

30Vol% clean glass fabric	Permittivity εr (40°C - 50Hz)	Dielectric dissipation factor tan δ (40C - 50Hz)
ML	4,43	$3,06E^{-3}$
Atlas 1/7	4,28	$2,36E^{-3}$

Table 13: Dielectric properties of laminates made with the reference epoxy resin (CY225/ 80phr HY925)

The flexural properties were measured for the epoxy reference with 30vol% of clean glass fabric (ML Y-direction and Atlas 1/7). For the ML and the Atlas 1/7 glass fabrics, the flexural strength is 451 and 450 MPa respectively and the flexural modulus is 12 and 12,57GPa. The density was also similar with 1,60 for the epoxy with ML fabric and 1,59 for the epoxy with atlas fabric. The flexural properties are similar for the two different kind of fabric. These results are coherent because the atlas fabric and the ML (Y-direction) are using the same material in that direction (EC9-68) and almost the same thread (Page 24, Figure 18 and Table 6).

30Vol% clean glass fabric	Flexural strength (MPa)	Flexural modulus (GPa)	Density (g/cm3)
ML (Y-Direction)	451 ± 20	12 ± 0,3	1,6
Atlas 1/7	450 ± 40	12,6 ± 0,6	1,6

Table 14 : Flexural properties and density of laminates made with the reference epoxy resin (CY225/ 80phr HY925)

Interlaminar shear measurements are made by short beam testing according to ISO 14130 and ASTM D2344. Tests are performed with 3mm thick plates with 30vol% of UD glass fabric. Plastic deformation was observed first which does not correspond to an interlaminar shear failure. It has been shown in the literature that increasing the volume percent of fiber in the laminates decreases the interlaminar shear strength and makes the failure more apparent (21). A plate with a thickness of 3mm is prepared with 60vol% of UD glass fabric by wet lay method. In the literature, ISO14130 and ASTM 2344 have been used to measure interlaminar shear of nanofilled laminates; an increase in the interlaminar shear strength has been observed with the addition of DGEBA resin.

The samples sized from the standard ISO 14130 exhibit delamination; although the delamination does not reach the outer edges of the samples as described in the standard. Samples prepared by ASTM D2344 show apparent delamination to the sample edges (Figure 32). The reference resin is transparent, thus delamination is easily observed. 60vol% UD laminates exhibits a maximum strength of 588MPa ±12 as measured by ISO 14130 and 595MPa ± 15 by ASTM D2344. Similar values from both standards allow us to conclude, that the ASTM D2344 sample from both standards have experienced delamination (Table 15).

UD Köper 1/3	Flexural strength (MPa)	Shear strength (GPa)
30 Vol% - ISO 14130	548 ± 30	55,6 ± 3,0
60 Vol% - ISO 14130	588 ± 12	63,5 ± 1,2
60 Vol% - ASTM D2344	595 ± 15	64,6 ± 0,4

Table 15: Mechanical properties of the epoxy resin (Reference) with UD Köper glass fabric

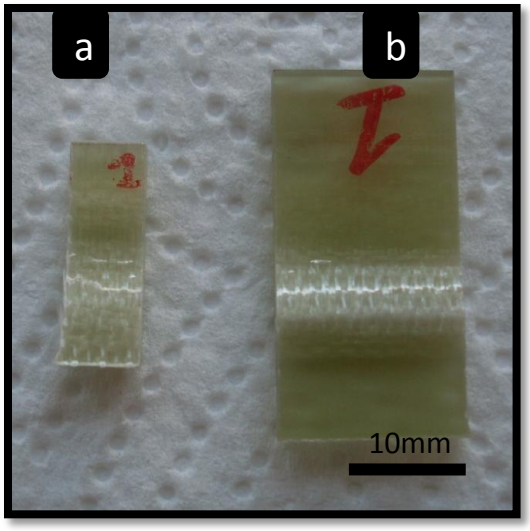

Figure 32 : Samples with 60vol% UD glass fibers after testing with the short beam method - a: ASTM2344 - b: ISO14130

5.3. Particle P1 (700nm)

Particle 1 is an ultrafine powder with an average diameter of 700nm and a surface area of approximately 20m²/g. Following the data sheet from the supplier, P1 particle is a good thermal conductor and electrical insulator and exhibits a low dielectric constant/loss. In the previous report (1), 10wt% of P1 particles mixed in the reference epoxy was found to be the highest concentration appropriate for injection molding. This concentration will be kept for the rest of the project.

1mm thick casted plates of 10wt% P1 particles in the reference epoxy are characterized with 3-points bending mode by DMA. The resulting data from the spectra (Spectrum 3) are summarized in the Table 16. In dual cantilever mode, the storage modulus at 40°C is 575MPa and the maximum of loss modulus is 150MPa at 110°C. The Tg (tan δ) is found at 113°C which is lower than the Tg measured with DSC (1). The storage moduli from dual cantilever and 3-points bending increase of 20% and 16% at 40°C and 10% and 57% at 140°C respectively compared to the reference resin. Below Tg, The particles are like physical crosslinks in the epoxy molecular chains in the composite. Above tg, the soft rubbery nature of the matrix makes the stiffness decrease dramatically contrary to the stiffness of P1 particles which stays constant. In the case of a polymer matrix filled with particles will make the nanocomposite stiffer above Tg.

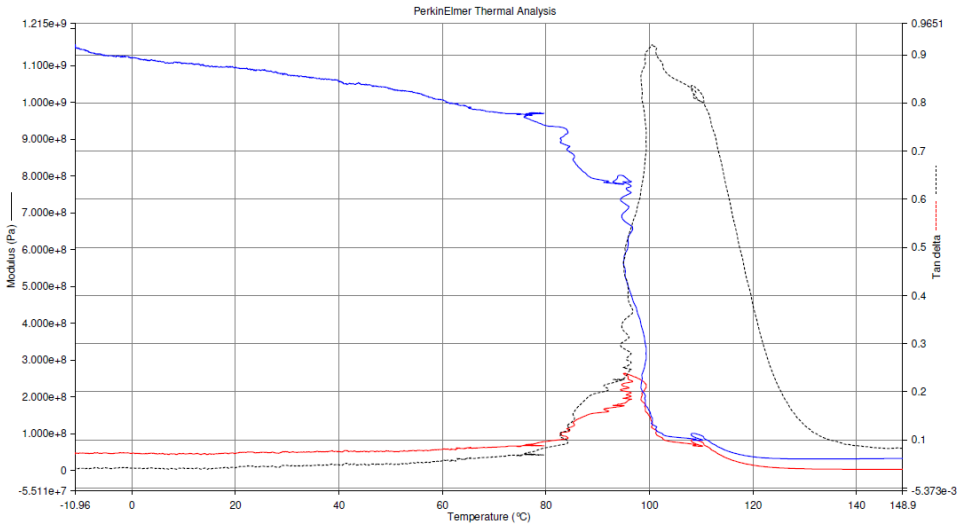

Spectrum 3 : Dynamical mechanical properties for 3points bending of a plate with a thickness of 1mm of the matrix with 10wt% PARTICLE 1 (700nm) F:100mN

3-points bending	Storage modulus			Loss modulus	Maximum loss modulus	Tg (tan δ peak)
Temperature	40°C	80°C	140°C	40°C	95°C	105°C
MPa	1056	940	33	50	266	

Table 16 : Dynamical mechanical properties for 3points bending of a plate with a thickness of 1mm of the matrix with 10wt% of P1 particles - F:100mN

The dielectric permittivity of the laminates with 10wt% of P1 is measured at 50Hz, ε_r is 4,54 for ML cleaned fabric and 4,5 for clean Atlas 1/7 glass fabric at 40°C. The dielectric dissipation factor is $3.23E^{-3}$ for ML clean fabrics and at 40°C and $2.82E^{-3}$ for Atlas 1/7 clean fabric; Tan δ is measured at 50Hz. The matrix with 10wt% of PARTICLE 1 and the laminate with 30vol% of unwashed Atlas glass fabric have an expansion coefficient below Tg of $57,43.10^{-6}$/°C and 58,26 respectively which represents an augmentation of 1,45% (Figure 33).

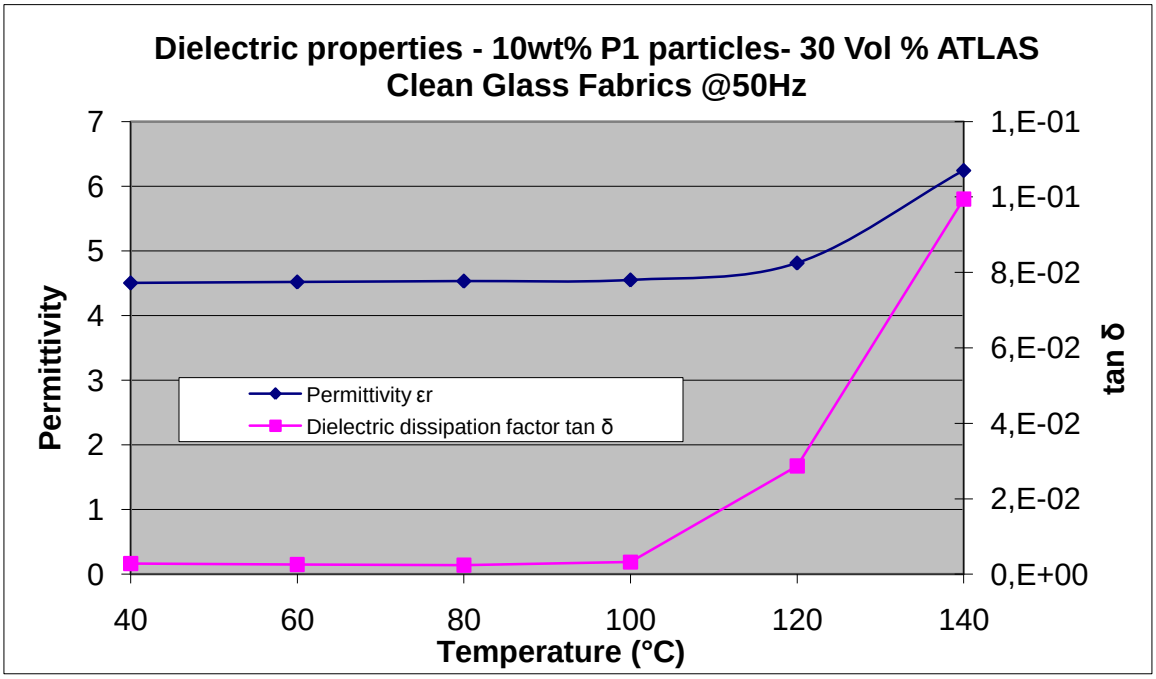

Figure 33 : Dielectric properties - 10wt% of P1 Particles - 30 Vol % ATLAS Clean Glass Fabrics @50Hz

The thermal expansion coefficient for the matrix with 10wt% of P1 particles is $57,43.10^{-6}$/°C which represents a reduction of 7,5% compared to the epoxy reference. The difference of thermal expansion coefficient between the matrix with P1 particles and the laminate with unwashed atlas glass fabric ($58,26.10^{-6}$/°C) is small (2%) compared to the laminate with 30vol% of atlas clean glass fabric whom the coefficient in greater of 7,3% with a value of $66,56.10^{-6}$/°C. (Table 17)

Flexural properties of laminates with P1 particles were measured with 30vol % of ML and ATLAS clean glass fabric. Flexural strength of laminates with ML (X and Y directions) and ATLAS are respectively 397MPa, 425MPa and 345MPa. Flexural modulus of laminates with ML (X and Y directions) and ATLAS are respectively 11,2GPa, 13,1GPa and 9,5GPa [Table 18].

The difference between the results of the two glass fabric is probably due the impregnation which was barely better with the ML fabric than with the atlas clean fabric.

For measuring flexural properties, the samples should not show difference between both sides (top and bottom). For P1 particles, the cross section reveals a layer of matrix with P1 particles only (Figure 34). Regarding the difference between the 2 sides of the samples (Figure 34), a bunch of sample with 30vol% clean glass laminate were tested one side (Resin at the bottom) and the rest in the other side. As we can expect, the best results were found with the sample

with the epoxy resin placed at the top because the maximum stresses are situated at the bottom of the sample. If the resin if situated at the bottom during the measurement, the resin will crack first and the material will exhibit a lower value of flexural strength.

P1 particles (700nm)	Thermal Expansion coefficient 10^{-6}/°C	Density (g/cm3)
Matrix	57,43	
Laminate with 30 Vol% Unwash ATLAS 1/7 fabric	58,26	1,65
Laminate with 30 Vol% clean ATLAS 1/7 fabric	66,56	1,63

Table 17 : Thermal expansion coefficient of epoxy resin with 10wt % of PARTICLE 1 (700nm)

Laminates with 10wt% P1 particles	Flexural strength (N/m2) MPa	Flexural modulus (Ef) GPa
Atlas 1/7 Clean glass fabric	362 ± 35	9.26 ± 0.53
ML Clean glass fabrics (Y-direction)	425 ± 29	13.12 ± 0.58
ML Clean glass fabrics (X direction)	397 ± 13	11.21 ± 0.51

Table 18 : Mechanical properties of laminates filled with 10wt% of PARTICLE 1

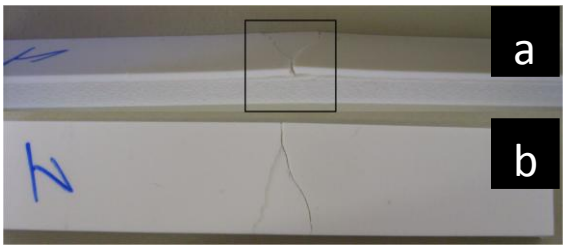

Figure 34 : Pictures of the test sample for flexural properties of laminate with 10wt% PARTICLE 1 and 30vol % clean Atlas 1/7 glass fabric a: Side, b:top

5.4. Particle P2 (70nm)

Particles P2 (P2) exhibit dielectric breakdown strength of 35kV/mm, high volume resistivity and thermal conductivity of 35W/m.K (data from the supplier). P2 has application to 1800°C in inert atmosphere, 1400°C in vacuum and 1000°C in oxidizing atmosphere. P2 particles are often used as a lubricant instead of graphite.

A TGA measurement is made to confirm the masterbatch particle concentration. For the future calculation, the concentration of Particle 2 in the masterbatch is 41wt%.

data	Wt% of residue at 800°C
From the supplier	41.6
From ABB	40.8

Table 19 : TGA measurements of the masterbatch with Particles 2 (70nm)

The viscosity of the masterbatch of 41wt% P2 (70nm) in EPON 828 is measured without and with dilution using the reference resin system (Figure 35 and Table 20). The maximum viscosity which is acceptable for impregnation is 1.5Pa.s at 65°C. As it was expected, the viscosity increases as the concentration of particles increases. For a concentration up to 20wt% the viscosity decreases as the temperature increases. For concentrations of 23 and 27wt% the viscosity decreases until 50 to 55°C and then increases again. The highest concentration appropriate for our setup is 20wt% (45.2phr) of P2 (70nm).

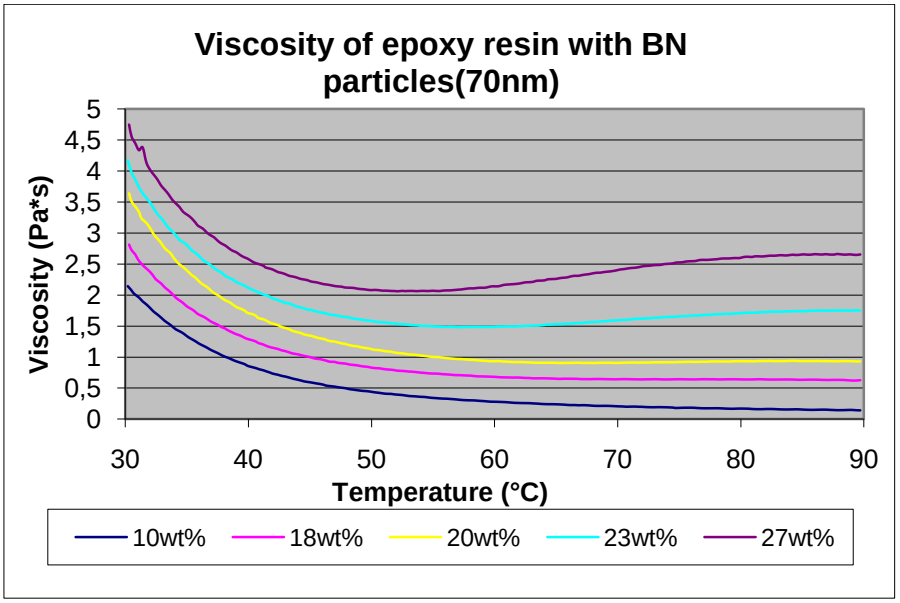

Figure 35 : Viscosity of epoxy resin with P2 particles (70nm) in function of the temperature and concentration

Viscosity at [Pa*s]:	65°C
P2 10wt% 20phr	0.24
P2 18wt% 39.7phr	0.65
P2 20wt% 45.2phr	0.91
P2 23wt% 54phr	1,5
P2 27wt% 67phr	2,3

Table 20 : Viscosity of the system with P2 (70nm) particles at 65°C

The Tg of the matrix material decreases as the amount of P2 particles increases, especially for concentration greater than 18wt% while the temperature of reaction remains constant at 170°C as measured by DSC. The exothermal enthalpy of reaction (ΔH) decreases as the concentration of P2 increases (Table 21). The decrease of Tg compared to the neat epoxy is due to the diminution of the crosslink density of the polymer when the P2 particles is added. The exothermic character of the curing reaction decreases significantly as the filler content increase (Table 21). The diminution of the exothermic reaction can lead to a lower shrinkage stress and internal mechanical stress of the matrix during processing and improved the used

with glass fibers. It is important to notice that the exothermic reaction of the epoxy in the composite stays the same, whatever the concentration of fillers is, only the amount of reactive material decrease and makes the exothermic reaction lower with fillers. The T_d and the char residue are measured by TGA. The T_d is not significantly affected by the content of particles. The char residue increases as the concentration of particles increased (Spectrum 4).

Epoxy resin with P2 particles

Wt% of BN Particles	T_d (°C) 99%/95%	ΔH (J/g)	$T_{reaction}$ (°C)	T_g(°C)
10wt%	328/367	236.5	168	117.96
18wt%	308/355	196.4	171	118.48
20wt%	310/362	174.35	169	111.16
23wt%	310/363			110.12
27wt%	304/366			

Table 21 : DSC and TGA measurements for P2 (70nm)

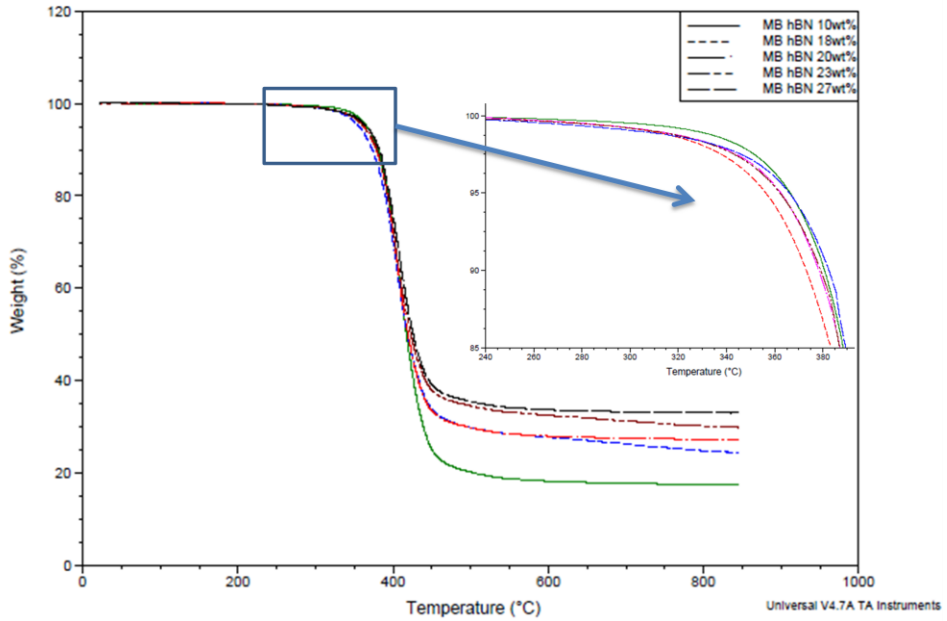

Spectrum 4: TGA of system with P2 (70nm) at different concentrations

P2 particles with an average diameter of 70nm appear as agglomerated flakes as observed SEM (Figure 36a and b).

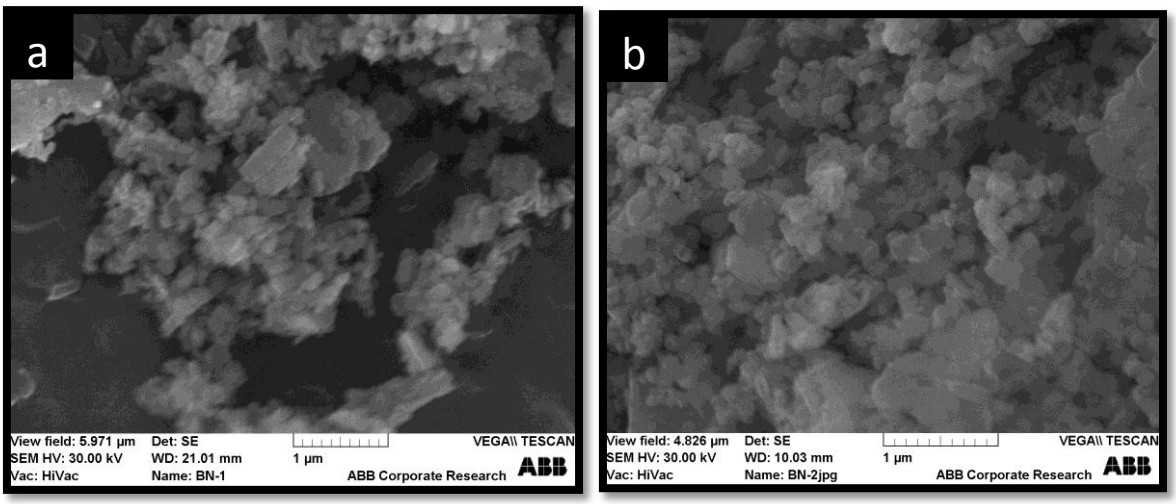

Figure 36 : a and b: SEM Picture of powder of P2 particles

The dispersion of P2 (70nm) particles in the matrix and laminates is examined by SEM (Figure 37 and Figure 38). The dispersion of the particles in the matrix is good, only some agglomerates of several micrometers are still visible (Figure 37a). Small particles are observed in high magnification pictures around agglomerates (Figure 37a). The particles are observed between the bundles of glass fabrics (Figure 38a). The dispersion is also optimized inside the bundles of glass fiber laminates as the particles are easily visible in the high magnification pictures (Figure 38b & c).

Low magnification *High magnification*

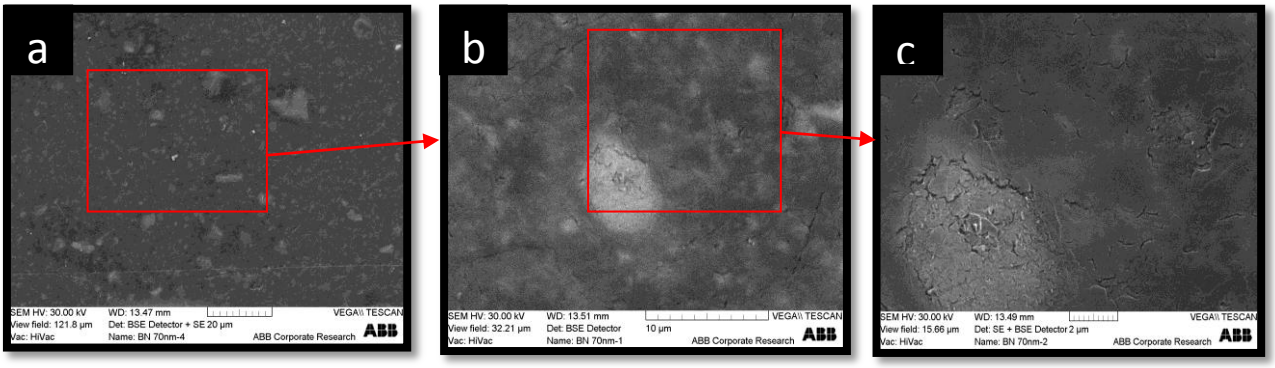

Figure 37 : SEM picture of 18wt% P2 filled epoxy resin

Low magnification *High magnification*

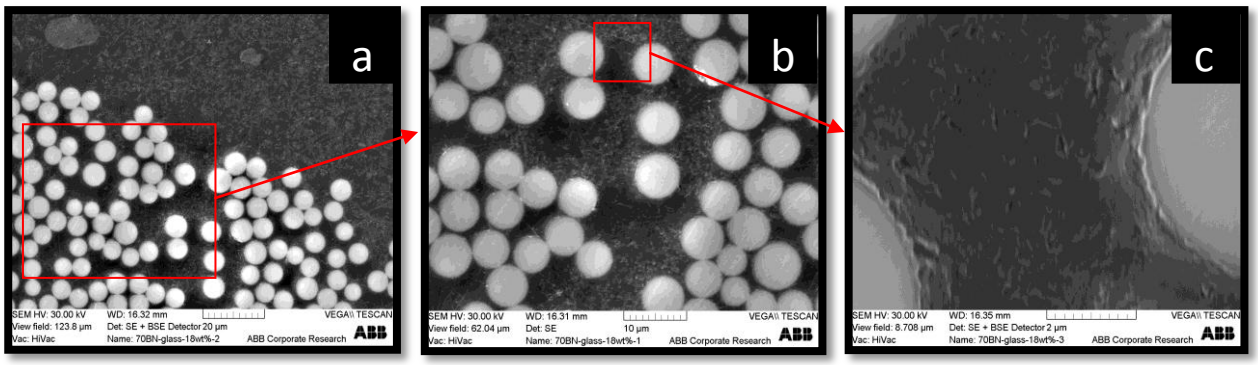

Figure 38 : SEM picture 18wt% P2 reinforced epoxy resin with 30 vol% cleaned ATLAS 1/7 glass fabric

1mm thick plates are characterized with 3-points bending mode by DMA. The resulting data from the spectra (Spectrum 5) are summarized in the Table 22. The Tg (tan δ) is found at 105°C which is lower than the Tg measured with DSC (111°C - Table 21). In 3-points bending mode, the storage modulus at 40°C is 1182MPa and the maximum of loss modulus is 287MPa at 95°C. The Tg (tan δ) is found at 100°C which is lower than the Tg measured with DSC (111°C - Table 21). The storage modulus from 3-points bending increase of 31% at 40°C and 124% at 140°C respectively compared to the reference resin. The impact of the P2 particles over the stiffness of the material is important especially above the Tg when the polymer matrix becomes softer.

3-points bending	Storage modulus			Loss modulus	Maximum loss modulus	Tg (tan δ)
Temperature	40°C	80°C	140°C	40°C	91°C	100°C
MPa	1182	957	47		287	

Table 22 : Dynamical mechanical properties for 3points-bending of a plate with a thickness of 1mm of the matrix with 20wt% of P2 particles

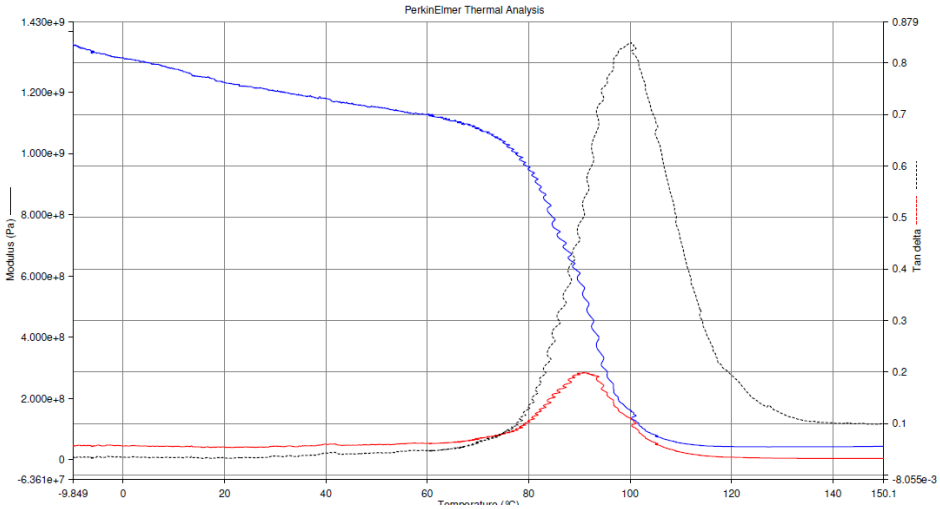

Spectrum 5 : 3-points bending - DMA of 20wt% P2 at a heat rate of 5°C/min and a dynamic force of 100mN and a heating rate of 5°C/min

System with 20wt% of P2 (70nm) is cast to evaluate the thermal, mechanical and dielectric properties of the nanocomposites. Unfortunately, the injection of 20wt% P2 particles (70nm) into clean atlas fabrics showed stripes of the neat resin on the surface of the laminate. A second laminate is prepared and similar stripes were observed but to a lesser extent. The plate is cut and the cross section observed by an optical microscopy to see how deep these stripes penetrated (Figure 39). The stripes of neat resin are only on the surface over the first fabric layer. A laminate of 30vol% of clean atlas 1/7 is impregnated with 18wt% P2 (70nm). The resultant laminate contains some stripes on the surface but to a lesser extent than previously observed. The fabrics were partially compressed and in one side of the laminate, 1mm of the thickness was only matrix like it has been observed with Particle 1.

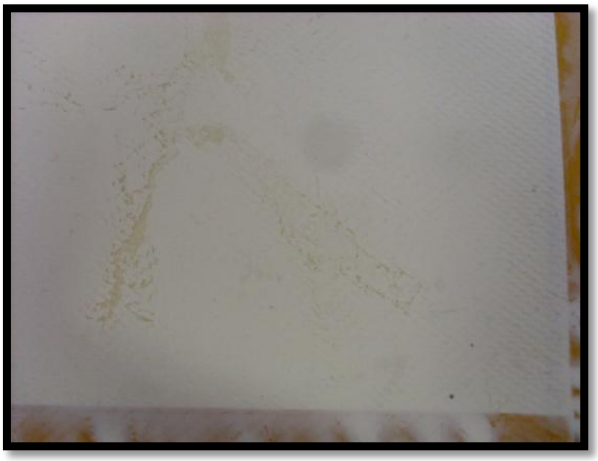

Figure 39 : Stripes on the small plate with 18wt% P2 (70nm) and 30vol% glass fabric

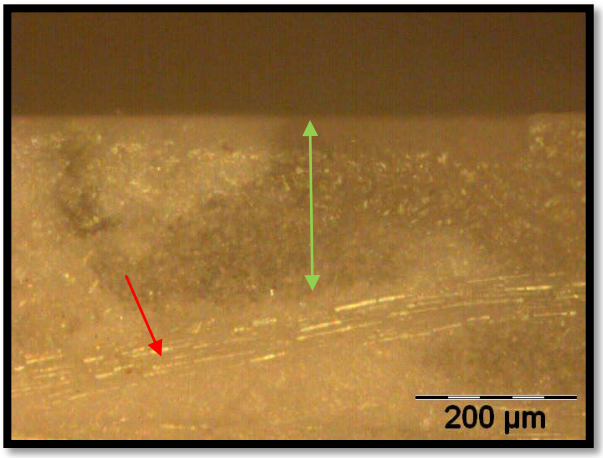

Figure 40: Stripes - Cross section of the P2 (70nm plate) Optical Microscopy – Red arrow: glass fibers, green arrow: stripes of resin

The dielectric permittivity of the resin matrix with 20wt% of P2 (70nm) is measured at 50Hz, ε_r is 3,71 at 40°C and increases to 4.35 at 120°C and 5.52 at 140°C. The dielectric dissipation factor is $3.68E^{-3}$ at 40°C and increases to a maximum of $6,55E^{-2}$ at 120°C; tan δ is measured at 50Hz. (Figure 41). The dielectric permittivity and the dielectric dissipation loss increase of 7% and 26% at 40°C. The dielectric permittivity of the resin with 20wt% of P2 (70nm) increases as a function of the temperature of frequency because of the dielectric polarization in the material at the interfaces matrix/particles. The dielectric dissipation factor for the temperatures between 40°C and 120°C decreases and stays almost constant after $4E^{+5}$ Hz. At 140°C and low frequencies, the dielectric dissipation factor decreases with a minimum at 20Hz and then increases again. The dielectric dissipation factor shows a maximum in the region of Tg because of the softening of the material which make of the orientation of large polar chain segments easier and a rise of the ionic conduction appears. Concerning the laminates with 18wt% of P2 and 30vol% clean Atlas E-glass fabric, the dielectric permittivity is measured at

50Hz, εr is 4,69 at 40°C and increases to 5,32 at 120°C and 5.52 at 140°C (Figure 42). The dielectric dissipation factor is 1,27E^{-3} at 40°C and increases to a maximum of 5,39E^{-2} at 120°C; tan δ is measured at 50Hz. The dielectric permittivity increases of 23% and the dielectric dissipation loss decreases of 57% at 40°C. The permittivity is higher for the glass reinforced resin than for the matrix while the dielectric dissipation loss decreases a lot.

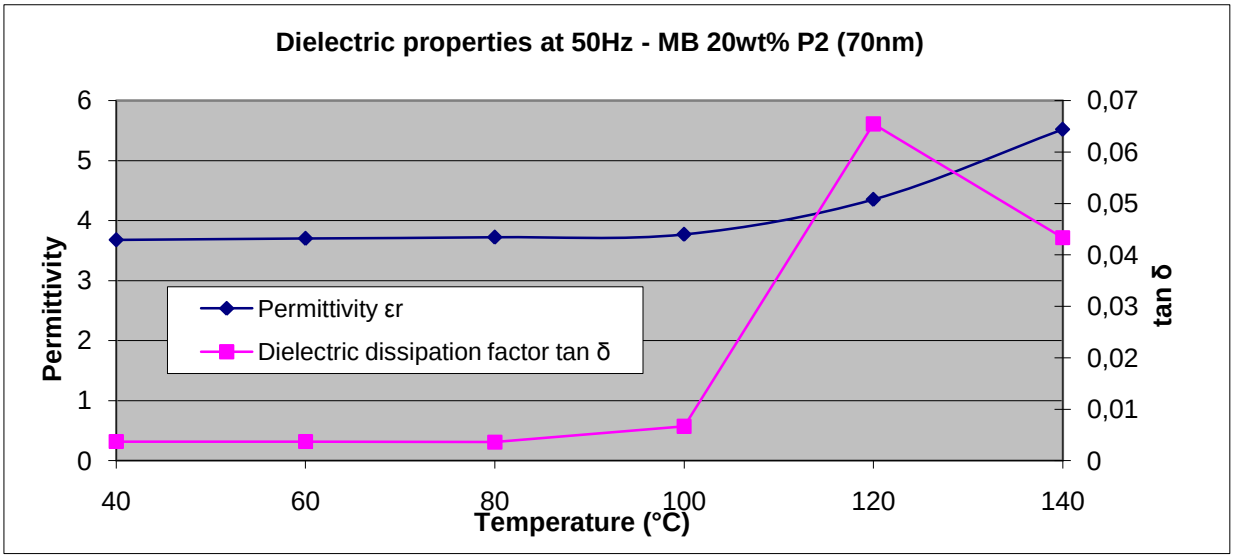

Figure 41 : Permittivity and dielectric dissipation factor for the matrix with 20wt% P2 (70nm) particles in function of the temperature at 50Hz

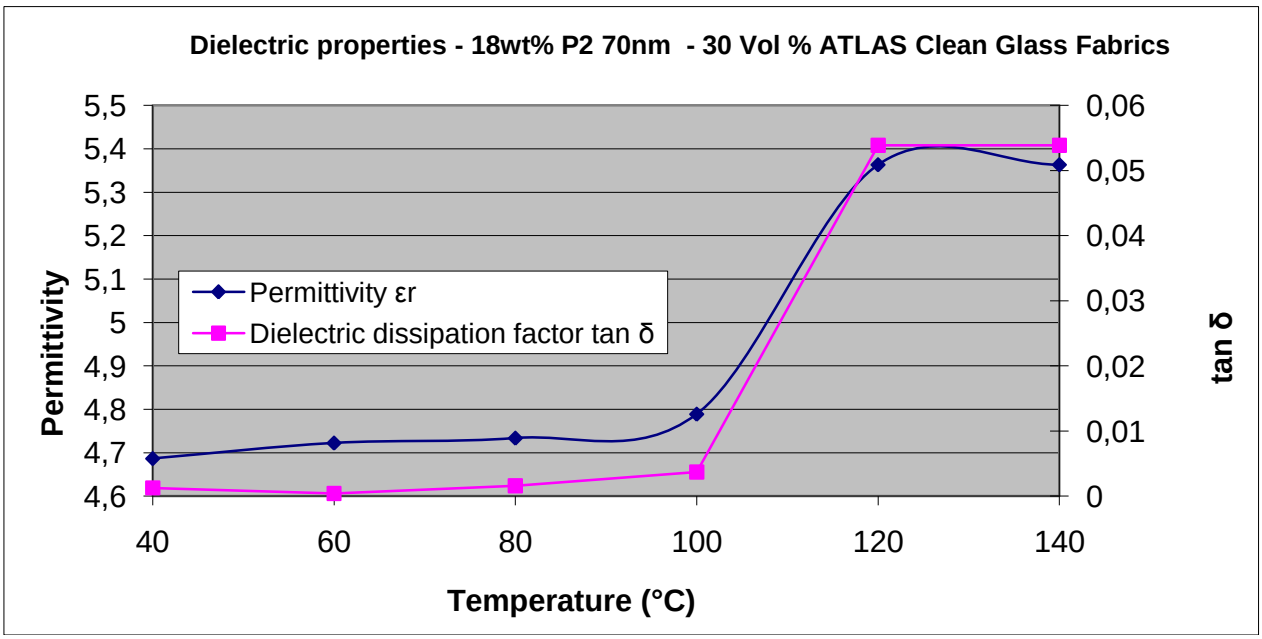

Figure 42 : Permittivity and dielectric dissipation factor for the matrix with 20wt% P2 (70nm) particles in function of the temperature at 50Hz

The thermal expansion above Tg of the matrix with 20wt% of P2 and the laminate with 18wt% of P2 and 30vol% of clean glass atlas 1/7 fabric is respectively 52,85 10^{-6}/°C and 67,24 10^{-6}/°C which is a reduction of respectively 15,4% and an increase of 8,29% . The addition of P2

particles decreases the thermal expansion coefficient because the P2 particles exhibit a lower value of this coefficient (1.10^{-6}/°C at 25 to 1000°C (44)) than the neat polymer matrix ($66,01.10^{-6}$/°C - Table 12). This reduction can also lead to a reduction of the resin shrinkage and thermal stress. For the laminate with clean glass fabric, the coefficient of thermal extension increases. The flexural strength of a sample with 20wt% (45.2phr) of P2 particles is measured to be approximately 99MPa and which is a decrease of 13.4% compared to the reference. The flexural modulus is 4.43 GPa which corresponds to a gain of 46% compared to the neat resin. The epoxy with P2 has a more brittle behavior than the reference.

Regarding the difference between the 2 sides of the samples (Figure 34), a bench of samples of 18wt% of P2 particles with 30vol% clean glass laminate were tested one side (Resin at the bottom) and the rest in the other side. As we can expect, the best results were found with the sample with the epoxy resin placed at the top. Indeed, in that case the maximum stresses are situated at the bottom of the sample. The flexural strength was 378MPa and the flexural modulus was 11.125GPa. If the sample is turned over and then tested, the maximum stresses undergo by the plate during the test are situated on the epoxy layer. The epoxy layer will break first, and then the rest of the plate which will falsify the results.

Sample **P2 particles (70nm)**	**Permittivity** ε_r (40°C - 50Hz)	**Dielectric dissipation factor tan δ** (40C - 50Hz)	**Thermal Expansion** 10^{-6}/°C (above tg) CTE	**Flexural strength** (N/m^2) MPa	**Flexural modulus** (E_f) GPa
Matrix 18wt%	3.68	3.71E-03			
Matrix 20wt%			52,85	99 ± 15	4.43 ± 0,04
Laminates 18wt% - 30vol% ATLAS 1/7 clean glass fabric	4,69	1.27E-03	67,24	378 ± 6	11.125 ± 0,051

Table 23: Dielectric and flexural properties of epoxy resins with P2 (70nm) particles

Conclusion Particle P2

The maximum viscosity admitted for VARTM is for 20wt% P2 particles (70nm) which is higher than Particle 1 whom the highest concentration was for 10wt%. SEM pictures showed in a previous report that the 10wt% P1 particles were found between and inside the bundles of fabric (1). For the laminates with 20wt% of P2 (70nm), the SEM pictures shows some agglomerates but also a good dispersion between the bundles, more SEM pictures and EDX analysis are necessary to study the dispersion inside the bundles of glass fibers. Concerning the storage modulus of the matrices measured by 3-points bending, matrix with 20wt% of P2 70nm shows an extent of 12% compared to the matrix with 10% Particle 1. P2 particles (70nm) exhibit a greater strength and flexural modulus of 4,4% and 20% than the Particle 1 (700nm) for

laminates with 30vol% clean atlas glass fabric. The dielectric permittivity of the laminates with clean atlas glass fabric with 10wt% of P1 and with 20wt% of P2 is measured at 50Hz, εr is 4,5 for Particle 1 and ε_r is 4,69 for P2 70nm at 40°C. The dielectric dissipation factor for laminates with 30vol% clean Atlas fabric at 40°C is $3.23E^{-3}$ for Particle 1 and $1,27E^{-3}$ for P2; Tan δ is measured at 50Hz. In one hand, the permittivity is higher for the glass reinforced resin than for the matrix but on other hand the dielectric dissipation loss decreases a lot and is even lower than the reference resin.

5.5. Particle P3 (100nm)

A masterbatch of 35,3wt% of P3 particle (100nm) in a modified bisphenol A is used for impregnation due to its low viscosity of 0,385 Pa.s at 65°C (1). 1mm thick plates of epoxy with 35,3wt% were characterized with 3-points bending mode by DMA. The glass transition temperature is measured from the phase angle and is determined between 102°C; Tg is lower that measured with DSC (122, 5°C (1)). The resulting data from the spectra Spectrum 6) are summarized in the Table 24. By 3-points bending mode, the storage modulus, measured as a function of temperature, shows a significant increase, it is 1170MPa at 96°C respectively. The storage moduli from 3-points bending increases by 29% at 40°C and by 105% at 140°C respectively, compared to the reference resin. The impact of the P3 particles over the stiffness of the material is significant especially beyond the Tg.

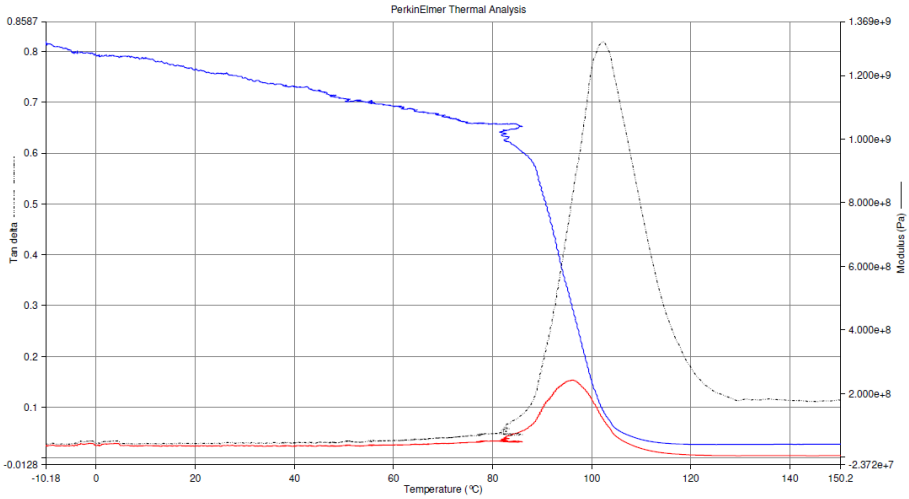

Spectrum 6: Dynamical mechanical properties for 3-points bending of a plate with a thickness of 1mm of the matrix with 35,3wt% P3 (100nm)

3-points bending	Storage modulus			Loss modulus	Maximum loss modulus	Tg (tan δ)
Temperature	40°C	80°C	140°C	40°C	96°C	102°C
MPa	1170	1050	43	33	245	

Table 24 : Dynamical mechanical properties for 3-points bending of a plate with a thickness of 1mm of the matrix with 35,3wt% P3 (100nm).

The dispersion of P3 (100nm) particles in the plate and the laminates with clean atlas glass fabric is examined by SEM. The particles are well-dispersed in the matrix and the laminates. It is difficult to distinguish the nanoparticles between the glass fibers at this magnitude but the surface looks similar to the Figure 43a where the particles are dispersed in the matrix.

Low magnification High magnification

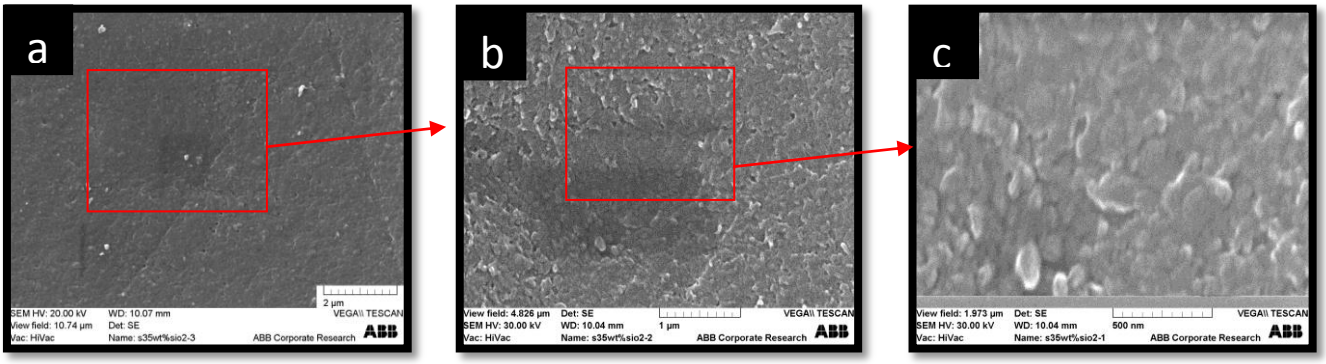

Figure 43 : SEM pictures - Matrix with 35wt% P3 (100nm)

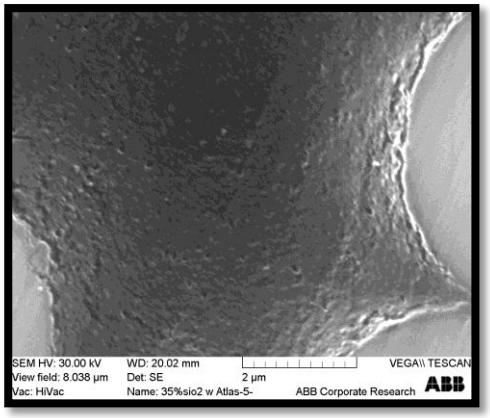

Figure 44 : SEM pictures - Laminates with 35wt% P3 (100nm) and 30 vol% cleaned ATLAS 1/7 glass fabric

The dielectric properties are measured for a 30vol% E-glass laminate with 35,3wt% P3 particles; the relative permittivity and the dielectric dissipation factor of laminates at 50Hz with 30vol% clean glass fabric are 4,79 and 3,71E^{-3} at 40°C (Figure 45). Regardless the frequency, higher is the temperature; more elevated is the relative permittivity. Compared to the other samples tested, laminates with P3 particles exhibits the highest value for dielectric constants which can be related to the important concentration of particles in the matrix, which creates more interfaces matrix/particle and an augmentation of the boundary layer polarization.

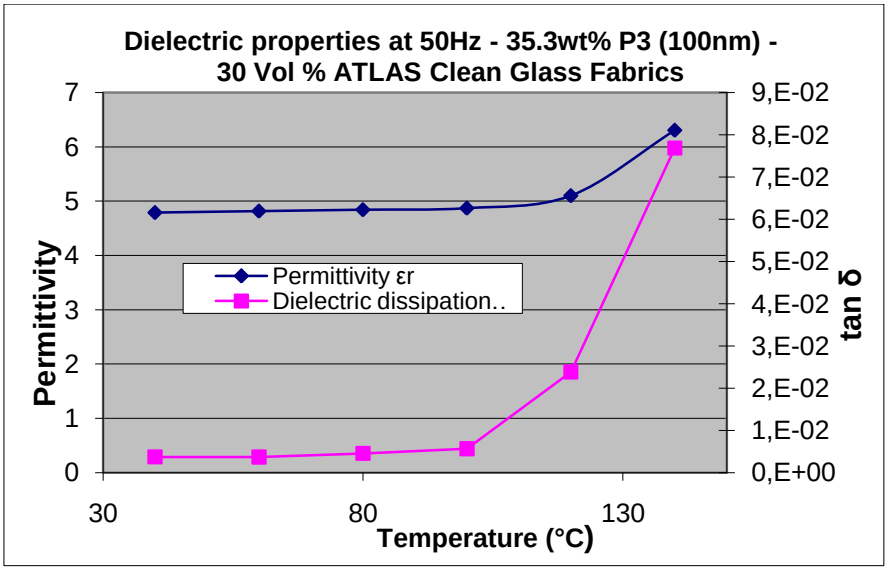

Figure 45: Dielectric properties at 50Hz for the 35,3wt% P3 particles composite epoxy resin with 30 vol% clean atlas fabric

In a previous report, the flexural strength and modulus of the matrix with 35,3wt% P3 particles were measured to 156,7MPa and 5053MPa respectively (1). The flexural strength and modulus of the laminates with 30vol% clean atlas 1/7 glass fabric are measured to be 469MPa and 13.4 GPa (Table 25). The thermal expansion coefficients are 44,34.10^{-6}/°C for the matrix; 43,52.10^{-6}/°C and 45,69^{-6}/°C for the laminate with respectively unwashed and clean fabric which represents a difference of -1,88% and +3% between the two coefficients and the matrix.

35,3wt% of P3 (100nm)	Flexural strength (N/mm2) MPa	Flexural modulus (Ef) GPa	Thermal Expansion 10^{-6}/°C
Laminate with 30 Vol% CLEANED ATLAS fabric	469 ± 30	13.4 ±2.0	45,69

Table 25: Flexural properties of the epoxy resin with 35,3wt% of P3 particles

35,3wt% P3 (100nm)	Thermal Expansion 10^{-6}/°C
Matrix	44,34
Laminate with 30 Vol% Unwashed ATLAS 1/7 fabric	43,52
Laminate with 30 Vol% clean ATLAS 1/7 fabric	45,69

Table 26 : Thermal expansion of the epoxy resin with 35,3wt% of P3 particles

Conclusion Particle P3

The impregnation of laminates with 35,3wt% of Particle P3 (100nm) was good without voids or heterogeneity. The laminates exhibit an important enhancement of the storage modulus and

of the flexural modulus compared to the neat resin. The dielectric properties are higher than the reference but stay acceptable considering the concentration of particles.

5.6. Particle P4 (45nm)

Particle P4 (45 nm) is examined due to its thermal conductivity of 26 W/mK (data from the supplier); the surface area is between 32 and 40m²/g and the density of Particle 4 is 3,6g/cm3 at 20°C. A 22.5wt% masterbatch in Araldit F is evaluated; the TGA of the masterbatch is measured to 800°C and the content of particles is determined to be 22,5wt% in agreement with the supplier. The masterbatch is mixed with the hardener and the accelerators described previously (Section page 26); the final concentration of particles is 12.8wt% in the system (Table 27). The viscosity of this blend is measured to be 0.255 Pa*s at 65°C (Figure 46) and is lower than the limit defined for the RTM setup (1). A curing cycle of 80°C for 6hours and 130°C for 10hours is used; the cured matrix has a Tg of 108°C as measured by DSC. Impregnation of the laminates is enhanced by the low viscosity of the resin system; the laminates surface appears homogenous without stripes.

Material	Initial %wt of particle	Td @ 99%(°C)	Td @ 95%(°C)	weight remaining (%) after 800°C
MB 12.8wt% P4	12.8	317.59	360	19.39

Table 27 : TGA of the matrix with 12,8wt% of P4 particles

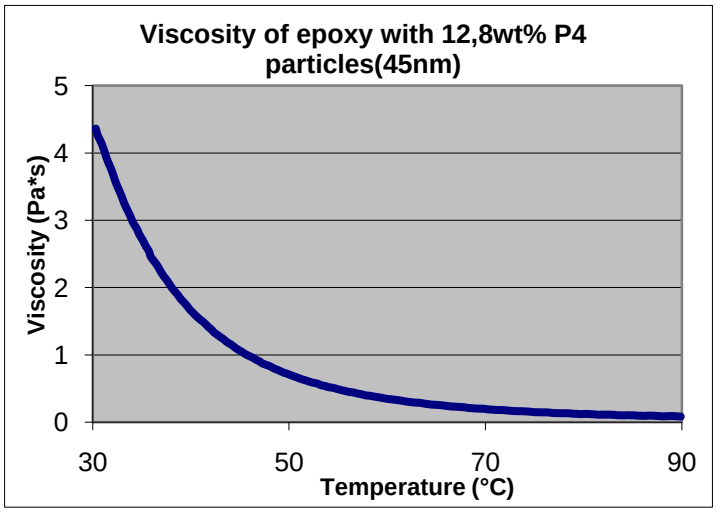

Figure 46 : Viscosity of the system with 12,8wt% of P4 particles (45nm)

The dispersion of P4 (45nm) particles in the matrix is examined by SEM (Figure 47). The dispersion in the matrix is good and no agglomerates are visible.

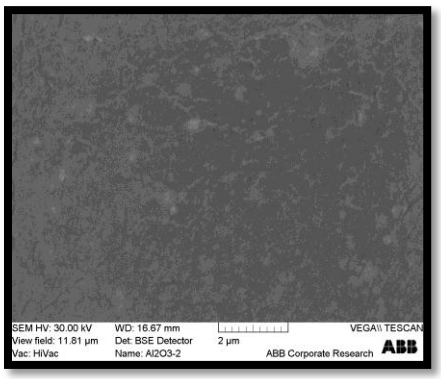

Figure 47 : SEM picture of the matrix with 12,8wt% P4

1mm thick plates of the matrix with 12,8wt% are characterized with 3-points bending modes by DMA. The storage modulus measured by 3-points bending mode at 40°C is 927MPa and the maximum loss modulus is 230MPa at 104°C (Figure 48 and Table 28). The Tg (tan δ) is found at 110°C which is higher than the Tg measured by DSC (Table 29).

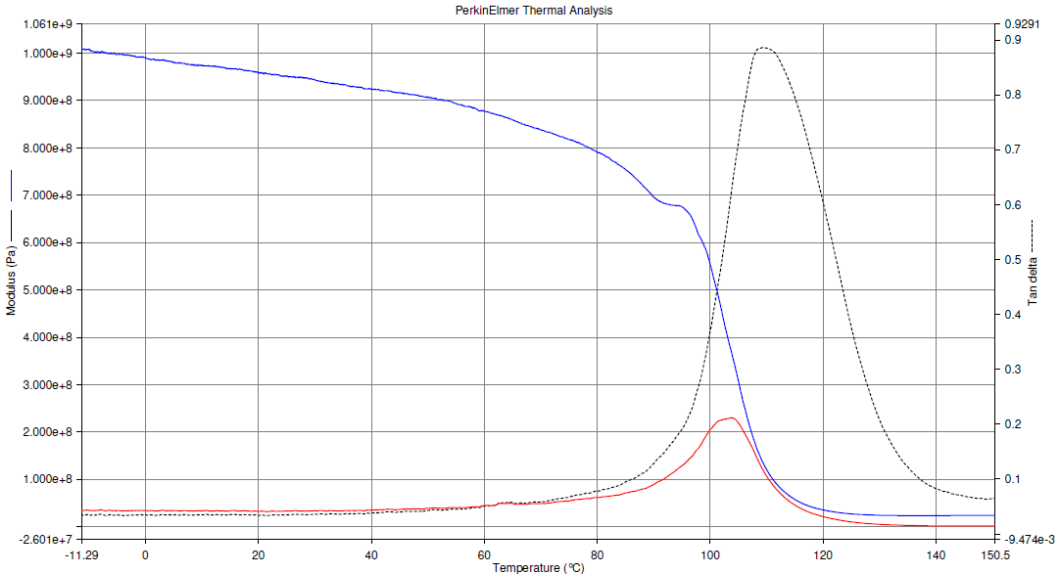

Figure 48 : 3-point bending - DMA of 12,8wt% P4 (45nm) at a heat rate of 5°C/min and a dynamic force of 100mN and a heating rate of 5°C/min

3-points bending	Storage modulus			Loss modulus	Maximum loss modulus	Tg (tan δ)
Temperature	40°C	80°C	140°C	40°C	104°C	107°C
MPa	927	790	27	37	230	

Table 28 : Dynamical mechanical properties for 3points-bending of a plate with a thickness of 1mm of the matrix with 12,8wt% of P4.

The permittivity of the matrix and the laminates with 30vol% clean Atlas 1/7 E-glass fabric at 40°C is 3,7 and 4,41 respectively at 50Hz (Table 29) which represents an increase of 19,2% for the laminates. The dielectric dissipation factor of the matrix and laminate at 40°C is

$4{,}19E^{-3}$ and $3{,}44E^{-3}$ at 50Hz respectively which represents a reduction of 17,9%. This reduction is encountered with all the materials tested previously.

The thermal expansion of the laminates is 62,24 10-6 /°C. The flexural strength of the matrix and laminates is 143 MPa ± 6 and 329MPa ± 46 respectively. The flexural modulus of the matrix and the laminates are 4.05 GPa ± 0,3 and 11,8GPa ± 0,5 respectively (Table 29).

Material **(MB P4 12,8wt%)**	Viscosity at 65°C [Pa*s]:	Tg(°C) DSC	Permittivity εr @40°C - 50Hz	Dielectric dissipation factor tan δ @40°C – 50Hz	Flexural strength (N/mm2) MPa	Flexural modulus (Ef) GPa	Thermal expansion (10^{-6} /°C)
Matrix	0.255	108.4	3.7	0.00419	143 ± 5.7	4.05 ±0.3	
laminates With 30vol% Atlas 1/7 cleaned glass fabric	-	-	4,41	0.00344	329 ± 46	11.8 ±0.5	62,24

Table 29 : Processing, electrical and flexural properties of the matrix and laminates with 12,8wt% of P4 particles (45nm)

Conclusion P4

Laminates with 12,8wt of P4 particles (45nm) filled epoxy was easily impregnated due to a low viscosity (0,255 Pa.s at 65°C) and exhibited no voids, filtering or cracks after impregnation by VARTM. No reference laminates was made with Araldit F. The electrical properties are still in a good range for the laminate and the matrix.

5.7. Particle P5 (15-30nm)

Particle P5 (P5) particles with an average diameter of 15-30nm have a thermal conductivity of approximately 30 W/mK g (data from the supplier). The P5 particles are amorphous and spherical with a true density of $3{,}4g/cm^3$and a surface area between 103 – $123m^2/g$.

A masterbatch of 40wt% of amorphous P5 dispersed in EPON® 828 is received; the highest concentration of particles dispersed in the cured system is 27wt% of particle with hardener (a dilution is incurred with the addition of hardener (HY925)). The received masterbatch is a powder which makes for difficulty in dispersion/mixing. Due to the density difference between the particle and the resin system, sedimentation of the particles is observed in samples of the cured system (Figure 49).

After an evaluation of different dispersion processes including high shear mixers and ultrasonic, it is determined that a maximum of 0,8wt% particles can be dispersed in the resin system without sedimentation during curing. The masterbatch is determined to be unfit for the impregnation of laminates by RTM or VARTM, although the wet-lay may be used to further evaluate this particle in a reinforced laminate.

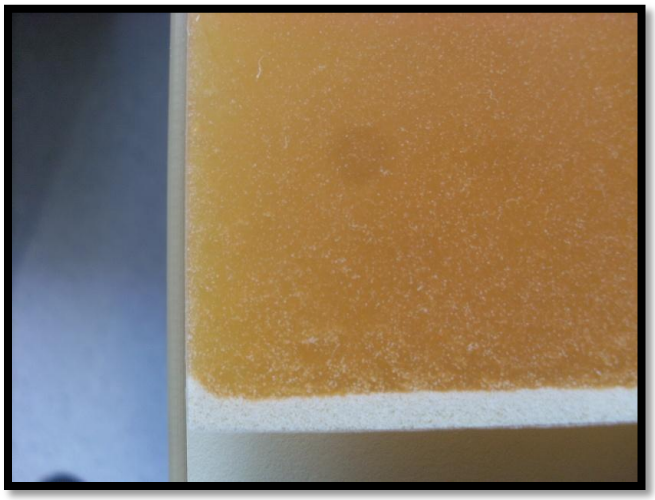

Figure 49 : Plate of 5wt% of P5 particles (15 - 30nm)

5.8. Electrical breakdown test

Electrical breakdown strength measurements of cast and laminate plates are examined by two techniques. Initial attempts used spherical electrodes with thin cast plate of epoxy; electrodes with a radius of 40mm are used to avoid field enhancement. According to the standard IEC 60243-1, the radius of the electrodes must be greater than 20mm. The cast sample plate is placed between the 2 spherical electrodes into a Gas insulated Switchgear (GIS) filled with SF_6 gas for testing. Both 4mm and 1mm thick sample plate are examined, a 4mm thick plate exhibited corona and electrical discharges so the experiment was stopped before electrical breakdown. Corona and discharges phenomena create disturbances on the scope, make the measurement impossible and can lead to a flashover. The breakdown strength of a 1mm plate of the neat reference is observed (Figure 50) once over the course of two experiments, unfortunately corona and electrical discharges were still observed and the results are considered unreliable. The corona and electrical discharges appeared at 22,63kV/mm and the electrical breakdown was at 27,58kV/mm. The breakdown path went straight through the plate, almost without cracks, only a small hole is visible at the middle of the plate, where the spherical electrodes were touching the plate (Figure 51).

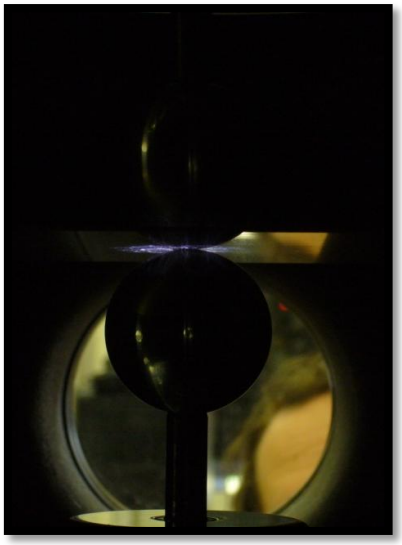

Figure 50 : First setup with neat resin plate - Corona and electrical discharges

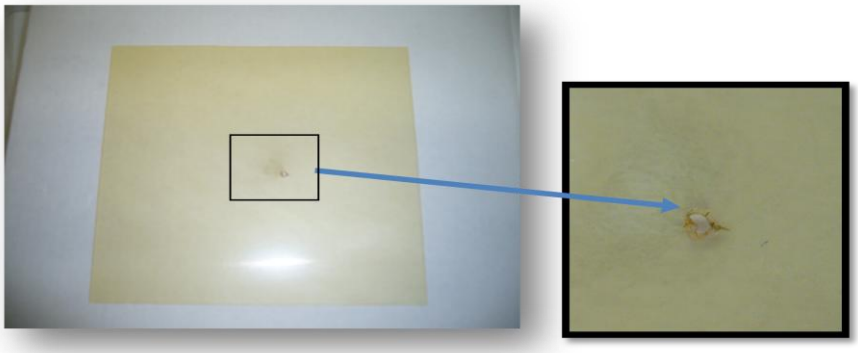

Figure 51 : Electrical breakdown of 1mm plate of neat resin

Based on the results of the tests using spherical electrodes, it is determined that the electrodes required further insulation in addition to gas. The second setup is composed two cylindrical electrodes and plates of 4mm only (with and without glass fabrics) where protective walls have been molded as described previously (Section Electrical breakdown samples, page 27 Figure 23). Surround walls are built in with epoxy around the electrodes to avoid flashovers. Cast or impregnate plates, prepared as described previously (Section Electrical breakdown samples, page 27, Figure 22) are placed between the two halves of the mold and the reference resin is injected to create walls. After curing the bottom and top of the sample are grinded for having flat surfaces to keep the maximum surface contact between the walls and the electrodes. Room curing epoxy resin is applied in order to bore the holes and the bubbles presented inside the wall. Finally, the sample is painted with silver paint inside of the wall (Table 7). Before electrical breakdown testing, the sample has to successfully pass partial discharges (PD) measurement.

Five samples with a plate made of the **reference resin**; the **reference resin with 30vol% clean Atlas 1/7 glass fabric** and the **35,3wt% of the P3 Particle** were selected and built following this procedure. Some samples more precisely with P3 particles and glass fabrics exhibit some important cracks after the curing and the cooling. Those samples are not proper for further tests because the cracks are weak points and will make the breakdown happening sooner (Figure 52).

Figure 52 : Samples for electrical breakdown test with an apparent crack (Walls: Epoxy reference, Plate: reference with 30vol% clean Atlas 1/7 glass fabric)

PD of those samples are measured. A sample is considered to be suitable for breakdown testing when the partial discharges do not exceed 20pC at 20kV. Each green dot represents a partial discharge. The intensity of the partial discharges depends on the size or the material of the defect (impurity, void, air bubble). A big defect will provoke a partial discharge with a high charge (Spectrum 7a) and will make a sample non-appropriate for electrical breakdown test. Small defects, for example at the interface between two different mediums, will provoke an important number of discharges but only with a low charge (Spectrum 7b) which make the sample still acceptable for electrical breakdown tests in our case.

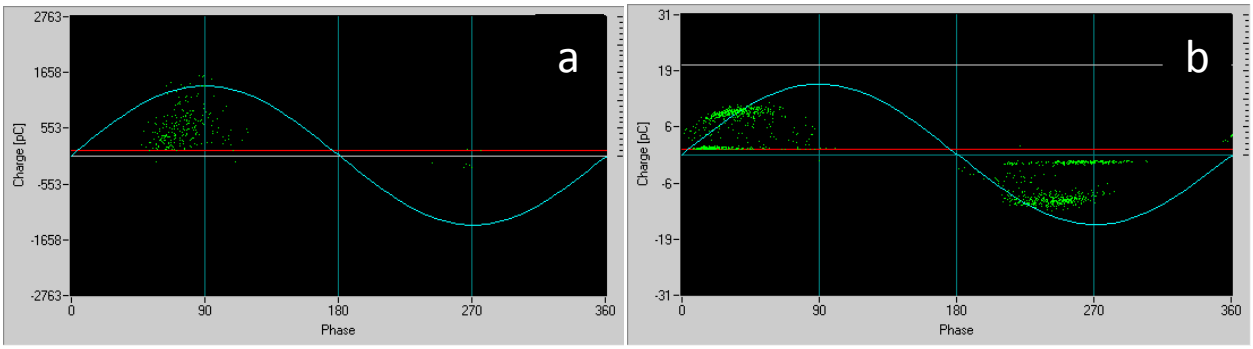

Spectrum 7 : PD measurements for clean glass fabric reinforced epoxy resin (reference) a: failed, b: passed

Results for electrical breakdown experiments are summarized in the Table 30.

In the first experiments, the breakdown happened at the border between the plate and the walls. This part is considered to be the weakest because when the sample is injected, usually some remaining air bubbles are still present. Moreover, molding injection around the plate creates sharp edges at this place. In that case the room temperature curing epoxy is applied to bore and smooth the edges. As described in many papers (45), the electrical breakdown path is growing in epoxy resin like a tree (electrical treeing) especially when particles or glass fabrics are added.

With the reference matrix, the electrical breakdown path went almost straight through the plate (Figure 53a). During the electrical breakdown, some cracks are produced around the main

electrical breakdown path (Figure 54). The electrical breakdown also travels through these cracks as some black burned materials are visible (Figure 55).

With the laminates, the electrical breakdown path did not go straight through the plate but have been barely following the glass fabrics (Figure 53b). The breakdown did not initiate cracks like it did with the sample without glass reinforcement. The cross section of a laminates after electrical breakdown is shown (Figure 56 and Figure 57). The electrical breakdown path is going through the resin, at the interface between the resin and the fiber. This part is considered to be the weakest in the composite because this part contains less bonding material and more voids compared to the glass fibers and the matrix. The dielectric strength of the air is lower than the dielectric strength of the epoxy resin and the E-glass.

The electrical breakdown path is clearly not going inside the bundles of glass fibers, but stays out of it. The black color corresponds to the resin which has been ionized and transformed in conductive carbon under the influence of the strong electrical field.

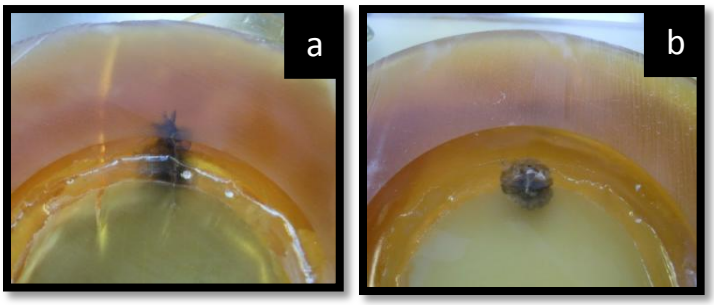

Figure 53 : samples after electrical breakdown test without the walls - Electrical breakdown trees - a: Reference resin only (R02), b: reference resin with 30vol% clean glass fabrics (GR01)

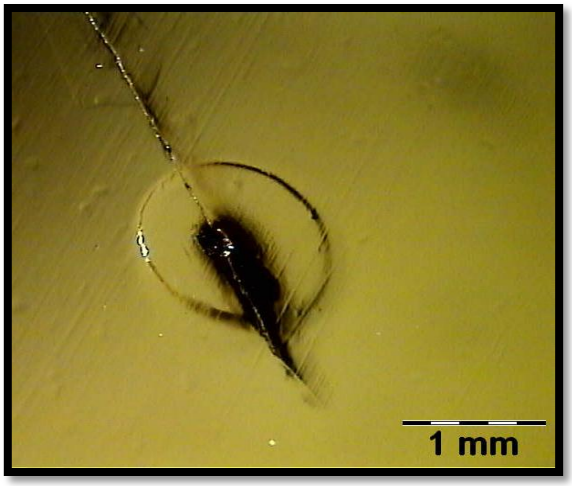

Figure 54 : picture of the upper part of the epoxy reference after electrical breakdown (Optical microscope)

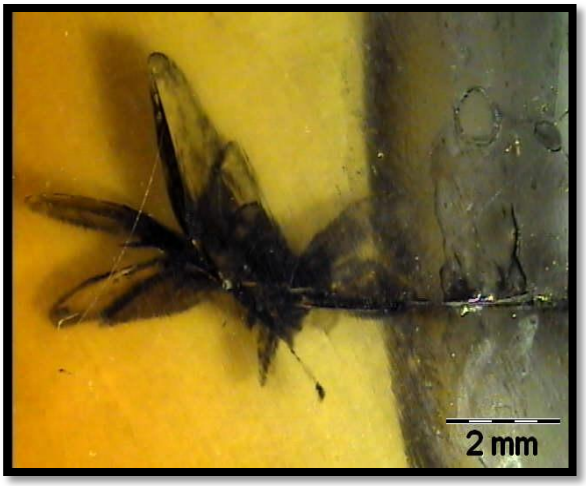

Figure 55 : picture of crack and electrical breakdown propagation of the epoxy reference after electrical breakdown (Optical microscope)

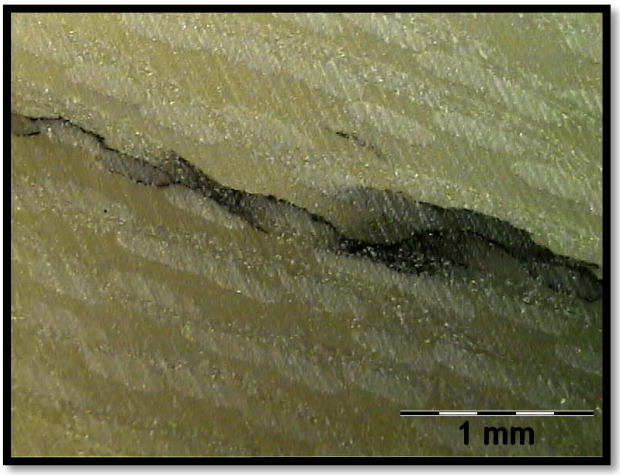

Figure 56 : Cross section of a laminate with the epoxy reference after electrical breakdown (Optical microscope)

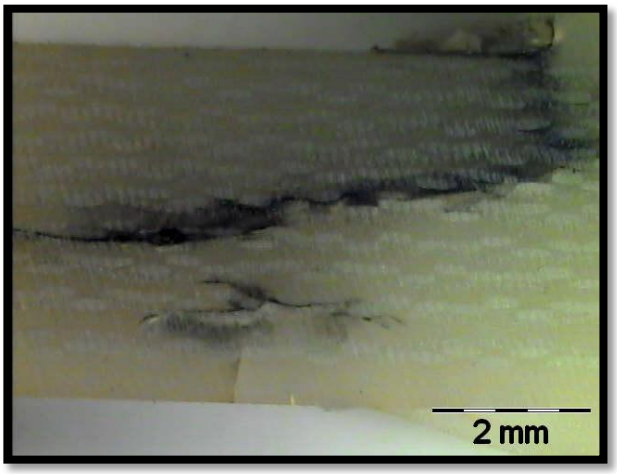

Figure 57 : Cross section of a laminate with the epoxy reference after electrical breakdown (Optical microscope - overview)

	PD measurement	<20pC at 20kV	Electrical breakdown Strength
Samples	pC at kV	Passed/Failed	V/mm (kV)
R01	800pC at 15.6kV		0
R02	800pC at 13kV		16,75
R03	300pC at 11kV		0
R04	<20pC at 20kV		0
R05	<30pC at 17.5kV		0
GR01	8pC at 17kV		19,53
GR02	30pC at 17.5kV		0
GR03	>500pC at 15kV		0
GR04	>100pC at 10kV		0
GR05	<20pC at 20kV		0
P3-01	<50pC at 15kV		0
P3-02	<20pC at 20kV		0
P3-03	<20pC at 20kV		0
P3-04	<50pC at 20kV		0
P3-05	<70pC at 20kV		0

Table 30: Data of electrical breakdown strength and PD measurements, R stands for the plates with reference epoxy resin matrix only, GR stands for laminates of reference epoxy resin with 30vol% clean glass fabric and P3 stands for the plates with 35,3wt% P3 matrix

Note: green colored samples are ready for breakdown testing, yellow could be improved with the silver-painting, red samples could be tested but maybe with early breakdown.

No further work was carried out at this stage; the samples are ready for electrical breakdown measurement.

6. CONCLUSION

This project was focused on studying the effects of particles on improving mechanical and thermal properties of clean glass fibers reinforced epoxy composites for electrical insulators. Epoxy layered submicro and nanosized particles composites based on diglycidyl-ether of bisphenol A and anhydride-curing agents have been synthesized. The particles examined in this report are Particle 1 (P1 – 700nm) supplied in powder; Particle 3(P3 – 100nm), Particle 2(P2 – 70nm), Particle 4 (P4 – 45nm) and Particle 5 (P5 – 15/30nm) supplied in masterbatches.

The first aim of this project was to characterize the thermal expansion and the dynamical mechanical properties of the epoxy reference which was 0,9GPa for the storage modulus at 40°C in 3-points bending. Laminates with 30vol% clean E-glass fabric and clean ML fabric were produced and the thermal expansion, dielectric properties mechanical properties were measured. Interlaminar shear strength of laminates of the epoxy reference with 30 and 60vol% uni-directional glass fabric was measured to be 55,6GPa and 63,5GPa respectively by the short beam method and ISO14130.

Complete studies of epoxy filled with P2 particles (70nm) and P4 Particles (45nm) were carried out and the matrix properties such as processing properties, microscopy, DMA, thermal expansion, dielectric properties and mechanical properties were measured. The particles were well-dispersed in the matrix and through the glass fibers. P2 particles in laminates exhibits a real improvement for the mechanical properties compared to the P1 particles, ten times bigger in diameter.

Laminates of epoxy filled with ceramic particles were studied. The dynamical mechanical analysis of all the particles was performed. Epoxies filled with 35,3wt% of P3 particles and with 20wt% P2 (70nm) show the best value with 1,17GPa and 1,18GPa respectively. Microcopy pictures of laminates were taken by SEM and optical microscope of P2, P3 and P4; the particles were well dispersed in the matrix and between the glass fibers. The thermal expansion coefficients decrease in function of the concentration of ceramic particles in the matrix, with 30vol% normal atlas 1/7 fabric, the thermal expansion tends to be between the value of the matrix with and without particles and with 30vol% clean atlas 1/7 fabric, the thermal expansion is measured to be less predictable. Dielectric properties were measured at 50Hz, the relative permittivity was always higher than the reference epoxy for the filled resins and more especially for laminates at 40°C. The laminates with 30vol% atlas 1/7 clean glass fabrics exhibit better results than the normal glass fabric. For the dielectric dissipation factor, the best results were measured for the laminates with 30vol% clean glass fabric, greater than the matrix only, the laminates with 30vol% of ML clean fabric and atlas 1/7 normal fabric. The flexural strength was measured, and the best results were found for the laminates with 30vol% atlas clean glass fabrics with 35,3wt% P3 particles and with reference epoxy. Concerning the flexural strength of the matrices, the most interesting were found to be 143MPa for the 12,6wt% P4 particles (45nm) but still a bit lower than the 35,3wt% of P3 particles (100nm) measured in a previous report (1).

Epoxy resin filled with P5 was not successfully yielded because the mixing of the masterbatch containing the particles was not efficient and exhibits agglomerates. No other study was carried out at this stage.

Because of some technical problems, it was not possible to measure the thermal conductivity of the matrices and laminates.

Electrical breakdown setup was built to test flat laminate of 4mm in a SF_6 gas chamber. Three types of samples were tested, samples with only matrix of the reference epoxy, samples with P3 particles filled epoxy plate and laminate of reference epoxy with 30vol% of clean atlas glass fabric. The preparation of the sample revealed to be very important because voids and air bubbles can make the electrical breakdown appears too soon and lower the electrical breakdown strength. The electric breakdown path follows the interfaces matrix/fibers.

7. Future directions/researches

As soon as the machine is fixed, the thermal conductivity of all the matrices and laminates should be measured.
The dispersion of the particles in the matrix and the laminates should be study deeper with SEM/EDX especially between the fibers in the bundle.
Short beam tests should be carried out in epoxy composite filled with particles to observe the affect of the particle on this value interlaminar shear strength.
Electrical breakdown could be performed with the other materials.
Other way to mix efficiently masterbatch with P5 particles should be explored such as high shear mixing and wet lay.

8. REFERENCES

1. **Peter Zweifel, Sian F. Fenessey.** *Advanced fiber reinforced composite – effect of micron and submicron fillers on the thermal conductivity and mechanical properties.* ABB Corporate research center (CHCRD - Baden-Dätwill - Switzerland) : ABB Technical report, 2010. Internal report 80334.
2. **May, Clayton A.** *Epoxy resins: chemistry and technology.* s.l. : M. Dekker, 1988.
3. **insulators, ABB composite.** www.abb.com/composites. [Online]
4. **Wichmann, M.H.G. et al.** *"Glass fiber reinforced composites with enhanced mechanical and electrical properties benefit and limitations of nanoparticle modified matrix.* s.l. : Eng Frac Mech 73 (2006) 2346, 2006.
5. **Haque.A, Shamsuzzoha.M, Hussain.F, Dean.D.** *S2-Glass/epoxy polymer nanocomposites: Manufacturing, structures, thermal and mechancial properties.* s.l. : Journal of composite materials, Vol 37, No. 20/2003, 2003.
6. **Kornmann, X. et al.** *Epoxy layered silicate nanocomposites as matrix in glass fibre reinforced composites.* s.l. : Comp. Sci. Tech. 65 (2005), 2259, 2005.
7. **Mahrholz, T. et al.** *Quantitation of the reinforcement effect of silica nanoparticles in epoxy resins used in liquid composite moulding processes.* s.l. : Comp. Part A. 40 (2009), 235, 2009.
8. **K. C. Yung, H. Liem.** *Enhanced thermal conductivity of boron nitride epoxy-matrix composite through multi-modal particle size mixing.* Hong Kong : Journal of Applied Polymer Science, Volume 106 Issue 6, Pages 3587 - 3591, 2007.
9. **Han, Z. et al.** *Thermal properties of composites filled with different fillers.* s.l. : IEEE International Symposium on Electrical Insulation (2008), 497., 2008.
10. *Thermal properties of composites filled with different fillers.* **Han, Z., Wood JM, Herman H, Zhang C, Stevens GC.** 497 - 501, s.l. : IEEE International Symposium on Electrical Insulation, 2008, Vol. 2008.
11. *Epoxy/h-BN composites for thermally conductive underfill material.* **Liang, Xiu, Wong.** pages 437 - 440, Atlanta (USA) : electronic components and technology conference 59th, 2009.
12. **Xingyi Huang, Pingkai Jiang, Chonung Kim, Qingquan Ke, Genlin Wang.** *Preparation, microstructure and properties of polyethylene aluminum.* s.l. : Composites Science and Technology 68 (2008) 2134–2140, 2008.
13. *Dielectric spectroscopy and partial discharge characterisation of fiber-reinforced epoxy materials.* **Page, A. Krivda and S.A.** ABB Corporate research center Baden-Datwill - Switzerland : XIIIth international symposium of high voltage engeenering, Netherlands 2003, 2003. ISBN 90-77017-79-8.
14. **Kochetov, R. et al.** *Preparation and dielectric properties of epoxy-BN and epoxy-AlN Nanocomposites.* s.l. : IEEE Electrical Insulation Conference (2009), 397, 2009.
15. **Zhao, H. et al.** *Effect of water absorption on the mechanical and dielectric properties of nano-alumina filled epoxy nanocomposites.* s.l. : Comp. Part A. 39 (2008), 602., 2008.
16. **Zhang, C. et al.** *Dielectric properties of born nitride filled epoxy composites.* s.l. : IEEE: Annual Conference on Electrical Insulation and Dielectric Phenomena (2006), 19, 2006.
17. **Dielectric Properties of Epoxy Nanocomposites containing TiO2, Al2O3 and ZnO fillers.** *J. C. Fothergill, J. K. Nelson, M. Fu.* UK : IEEE, 2004.

18. **Clyne, D. Hall and T.W.** *An introduction to composite materials.*
19. **14130:1997, Standard ISO.** Fibre-reinforced plastic composites - Determination of apparent interlaminar shear strength by short beam method. 1997.
20. **D2344, ASTM.** Standard test method for short-beam strength of polymer matrix composite materials and their laminates.
21. *On short beam shear tests for composite materials.* **al, Whitney et.** 1985.
22. *Study of three- and four-point shear testing of unidirectional composite materials.* **Admas, Ming Xie and Donald F.** 1994.
23. **Ashbee, Ken.** *Fundamental principles of fiber reinforced composites.* 1989.
24. **14129:1997, ISO.** *Fibre-reinforced plastic composites -- Determination of the in-plane shear stress/shear strain response, including the in-plane shear modulus and strength, by the plus or minus 45 degree tension test method.* s.l. : Standard ISO, 1997.
25. **94(2007), ASTM D3518 / D3518M -.** *Standard Test Method for In-Plane Shear Response of Polymer Matrix Composite Materials by Tensile Test of a ±45° Laminate.* 2007.
26. **Administration, US departement of transportation - Federal Aviation.** *Test methods for composites a status report - Volume 3 shear test methods.* 1993.
27. **1997, Von Leif A.Carlsson R. Byron Pipes.** *Experimental characterization of advanced composite materials Second edition .* s.l. : Technomic Publishing.
28. **ASTM.** *D5379 / D5379M (Standard Test Method for Shear Properties of Composite Materials by the V-Notched Beam Method.).* 1993.
29. **Melin, L. G., Neumeister, J. M., Pettersson, K. B., Johansson, H., & Asp, L. E.** *Evaluation of four composite shear test methods by digital speckle strain mapping and fractographic analysis. .* s.l. : Journal of Composites Technology and Research, 22(3), 161, 2000.
30. **J.S.Hawong, D.C. Shin, U.C. Baek.** *Validation of pure shear test device using finite element method and experimental methods, .* South Korea : School of Mechanical Engineering, 2003.
31. **Neumeister, J M, Palsson, A C.** *Inclined double notch shear test for improved interlaminar shear strength measurements.* s.l. : ASTM Journal of Composites Technology & Research (USA). Vol. 20, no. 2, pp. 100-107. Apr. 2008, 2008.
32. **7078-05, ASTM International D.** *Shear Properties of Composite Materials by V-Notched Rail Shear Method.* 2005.
33. **Adams, Dr Donald.** Shear test methods iosipescu vs v-notched rail. *High-Performance composites.* [Online] 01 2010. http://www.compositesworld.com/articles/shear-test-methods-iosipescu-vs-v-notched-rail.
34. **L.B. Manfredi, H. De Santis, A. Vázquez.** *Influence of the addition of montmorillonite to the matrix of unidirectional glass fibre/epoxy composites on their mechanical and water absorption properties.* Mar del Plata, Argentina : Composites: Part A 39 (2008) 1726–1731, 2008.
35. **Malte H.G. Wichmann, Jan Sumfleth, Florian H. Gojny, Marino Quaresimin, Bodo Fiedler, Karl Schulte.** *Glass-fibre-reinforced composites with enhanced mechanical and electrical properties – Benefits and limitations of a nanoparticle modified matrix.* Hamburg, Germany : Engineering Fracture Mechanics 73 (2006) 2346–2359, 2006.
36. **Imai, T. et al.** *Improving epoxy-based insulating materials with nano-fillers toward practical application.* s.l. : IEEE Electrical Insulation Conference (2008), 201., 2008.
37. **Deng S, Hou.M, Ye.L.** *Temperature-dependent elastic moduli of epoxies measured by DMA and their cotrrelations to mechanical testing data.* s.l. : Science direct, Polymer testing 26 (2007), 803 - 813, 2007.

38. **Vantico, Huntsman -.** *TDS Araldit casting resin system CY225/HY925/SiO2.* s.l. : Huntsman , 2000.
39. **group, suter swiss-composite.** katalog. *www.swiss-composite.ch.* [Online] 2010. [Cited: 02 14, 2010.]
40. **60270, IEC.** *High voltage test technique - Partial discharge measurements.* s.l. : International standard, 2000. IEC60270/2000(e).
41. **Reto Weder, Leo Ritzer.** *Vergleichende Untersuchungen an gereinigtem und ungereinigtem Hybridgewebe Polyester-Aramid (Kevlar) der Firma Tissa in Oberkulm.* Baden-Dätwill (CH) : ABB CH-RD V1 , 2008. ABB CH-RD V1 2008-848.
42. **Ashbee, Ken.** *Fundamentale principles of fiber reinforced composites.* 1988.
43. **Biron, Michel.** *Thermosets and composites.* s.l. : Elvissier, 2004.
45. *Electrical tree propagation along barrier-interfaces in epoxy resin.* **R. Vogelsang, R. Brütsch, T. Farr, K. Fröhlich.** Switzerland : Conference on Electrical Insulation and Dielectric Phenomena, CEIDP 2002, Cancun, Mexico, 2002.
46. **Manfredi, L.B. et al.** *Influence of the addition of montorillonite to the matrix of unidirectional glass fibre/epoxy composites on their mechanical and water absorption properties.* s.l. : Comp. Part A. 39 (2008), 1726, 2008.
48. **Gottfried W. Ehrenstein, Gabriela Riedel, Pia Trawiel.** *Thermal Analysis of plastics - Theory and practice.* s.l. : Hanser. ISBN 1-56990-362-X.
50. *Enhanced thermal conductivity of boron nitride epoxy-matrix composite through multi-modal particle size mixing.*

9. APPENDIX

9.1. Appendix : Electrodes design

A numerical analysis using a software was performed to validate the dimensions and shape of the electrodes and samples. Halves of the sample and setup are represented and used for calculation due to the symmetry. The electric field is represented using equilines (Figure 58, Figure 61 and Figure 64) and calculated along the edge of the electrodes (Figure 59, Figure 62 and Figure 65) and along the wall of the sample (Figure 60, Figure 63 and Figure 66). Three analyses were performed; analysis with a diameter of the lower edge of the electrode of 5mm and 10mm and a non-protruding plate; and an analysis with a diameter of the lower edge of 5mm and a protruding plate around the sample.
The equilines show the homogeneity of the electrical field on the plate between the electrodes and then, the equilines follow barely the shape of the upper part of the electrodes. In order to avoid flashover, the electric field must be highest at the triple point (point situated at the outer edge of the contact surface between the wall of the sample and the electrode). In the three studies, this fact is respected which means that the samples are suitable for electrical breakdown measurements. With a protruding plate, the electric field exhibit a field enhancement (peaks) at the sharpened edge of the plate but this value is still lower than the triple points of the setup.

Electric field – 5% equilines	*Along the edge of the electrode Field/meter – E=1kV*	*Along the edge of the electrode Field/meter – E=1kV*
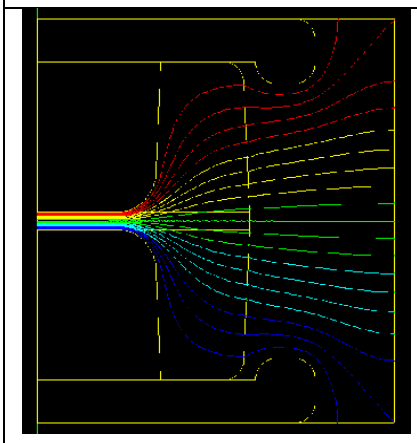	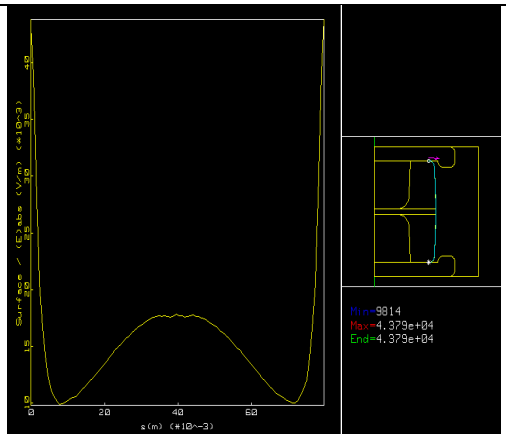	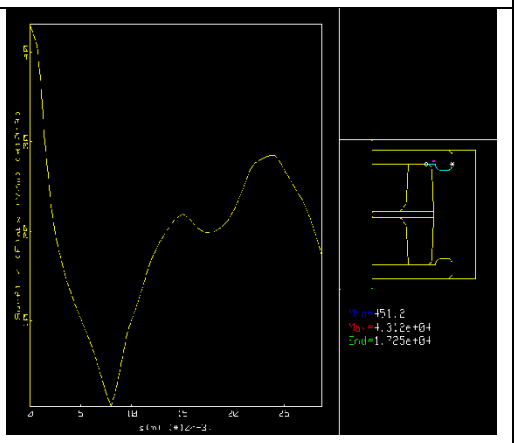
Figure 58 : electric field calculation for fiber reinforced material - electrodes with a radius of 5mm	**Figure 59 : Spectrum of the electric field along the walls - E=1kV - Radius=5mm**	**Figure 60 : Spectrum of the electric field along the edges of the electrode - E=1kV - Radius=5mm**
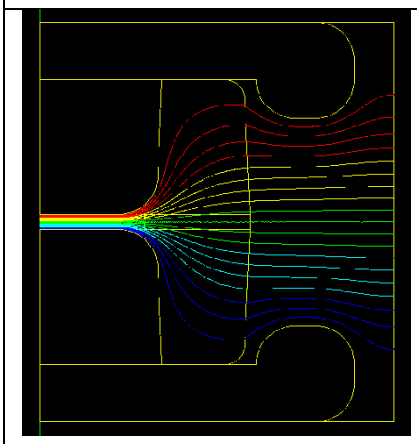	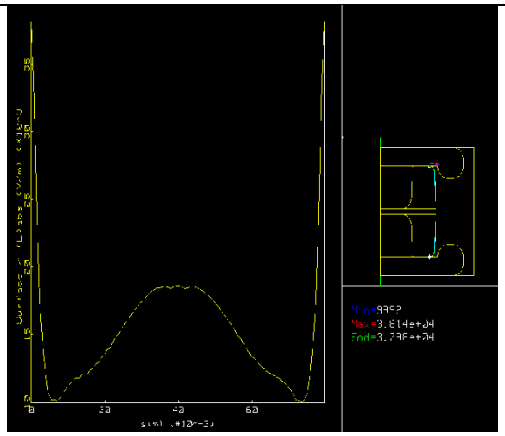	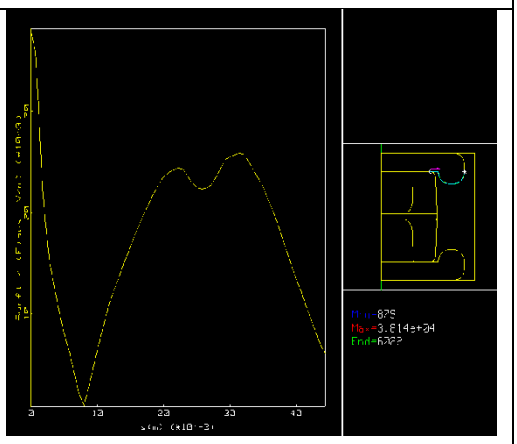
Figure 61 : electric field calculation for fiber reinforced material - electrodes with a radius of 10mm	**Figure 62 : Spectrum of the electric field along the walls - E=1kV - Radius=10mm**	**Figure 63 : Spectrum of the electric field along the edges of the electrode - E=1kV - Radius=10mm**
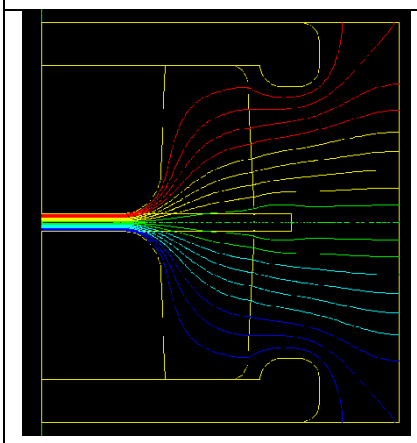	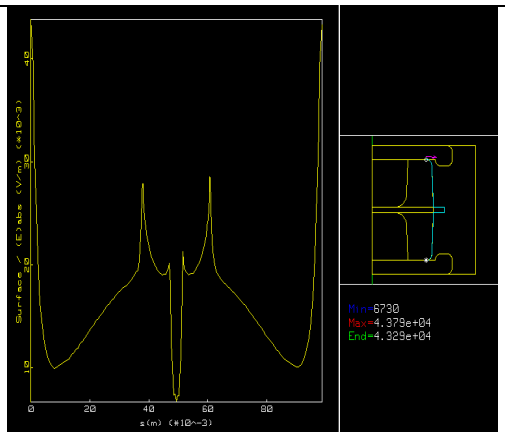	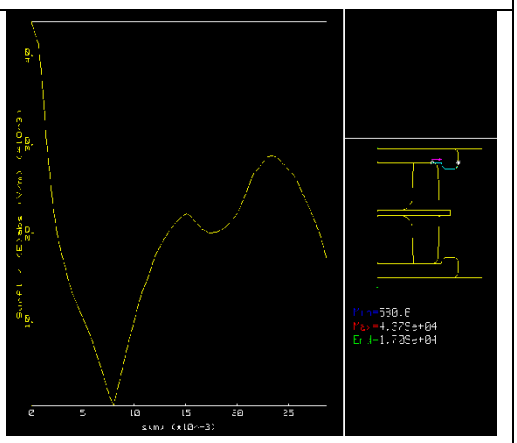
Figure 64 : electric field calculation for fiber reinforced material -	**Figure 65 : Spectrum of the electric field along the walls - E=1kV - Radius=5mm -**	**Figure 66 : Spectrum of the electric field along the edges of the electrode - E=1kV -**

electrodes with a radius of 5mm and a protruding plate	**Protruding plate**	**Radius=5mm Protruding plate**

9.2. Appendix : Thermal expansion

.

Thermal Expansion 10^{-6}/°C	Matrix	Unwashed ATLAS glass Fabric (30vol%)	**Clean ATLAS glass Fabric** (30vol%)
Neat resin	**62.09**	**66.01**	**44,34**
P3 (100nm) 35wt%	**43.52**	**44.34**	**45,69**
BN HCPL (27wt%)	**50.47**	**44.93**	**-**
BN (500nm) 18wt%	**52.37**	**56.3**	**-**
PARTICLE 1 10wt%	**57.43**	**58.26**	**66,56**
P2 (70nm) 18wt%	**52,85**	**-**	**67,24**
P4 12,8wt%	**-**	**-**	**64,30**

Table 31 : Coefficient of thermal expansion of some epoxy resin systems